This is a peer-reviewed, accepted manuscript of the following paper: Bhowmik, B. (2024). Advancements in online modal identification: a recursive simultaneous diagonalization comprehensive framework for real-time applications. Engineering Structures, 305, Article 117770. https://doi.org/10.1016/j.engstruct.2024.117770

Advancements in Online Modal Identification: A Recursive Simultaneous Diagonalization Comprehensive Framework for Real-Time Applications

Basuraj Bhowmik

[a] *Indian Institute of Technology (BHU), Varanasi, OSCAR Lab, Department of Civil Engineering, Varanasi, 221005, Uttar Pradesh, India*

Abstract

This paper introduces a recursive formulation of blind modal identification as an alternative to conventional diagonalization methods based on multi-lagged covariance matrices. While traditional blind source separation methods are effective for modal identification in structural systems, dynamic systems experiencing sudden changes or rapidly changing environmental conditions require real-time algorithms for continuous health assessment. The proposed recursive eigenspace updates on output covariance estimates, using generalized eigen perturbation, show promise in identifying modal parameters for numerically simulated systems excited with white and colored noise spectra. The paper presents a detailed framework based on recursive simultaneous diagonalization, avoiding real-time diagonalization of multi-lagged covariance matrices by incorporating two auto-covariance matrices with different lags. To evaluate the performance of the new real-time algorithm, synthesized data from a five-degrees-of-freedom system is used. A comparison with traditional independent components demonstrates the effectiveness of the proposed approach in separating closely spaced modes with high damping in real-time. Experimental investigations conducted on controlled vibroimpact test beds confirm the robustness of the proposed approach. Furthermore, the paper shows that the modal parameters obtained using the proposed method for the benchmark ASCE-SHM structure are consistent with those obtained from state-of-the-art methods. The examples presented in the paper indicate that real-time mode separation for dynamic systems in operating conditions is feasible, which is a novel contribution in the field of recursive simultaneous diagonalization.

Keywords: Real-time, online modal identification, generalized eigen perturbation, recursive diagonalization, benchmark structures

1. Introduction

A representative class of methods based on statistical signal processing – known as blind source separation (BSS) – dealing with the recovery of modes from response only data, has gained significant pre-eminence in recent times (Cichocki and Amari (2002); Hazra et al. (2009)). Despite its progress in terms of accuracy and robustness in mode separation, *real-time* modal identification using BSS still remains an unaddressed challenge, which is vital for systems exposed to continuously changing environments like sudden damages. Complex systems are susceptible to many types of anomalies, faults and abnormal behaviour – caused by a variety of subpar off-nominal environments – that may result in failures, unscheduled downtimes and catastrophic events. Early and accurate detection of these anomalies has become an active area of research and application in many domains as it can relate to significant, and often critical, actionable data-deriven decision-making in a wide variety of applications Chandola et al. (2009). Traditional BSS based modal analysis utilizes the system responses to extract mode shape matrix and the modal response. The use of BSS to separate individual modes from vibration based measurements provides a simpler alternative to other identification methods used in operational modal analysis (OMA) even in presence of higher damping ((Zhou and Chelidze, 2007)). As conventional parametric identification techniques such as stochastic subspace identification (SSI) Skolnik et al. (2006), eigen system realization (ERA) (Juang and Pappa (1985)), and natural excitation technique (NExT) (James et al. (1995)) pose serious identification issues for time-varying systems (e.g. tuned mass dampers that are frequently prone to mistuning), continuous online monitoring for infrastructures becomes essential. Of a wide gamut of BSS techniques for modal identification, algorithms based on SOBI (second-order-blind-identification), relying on joint diagonalization are most popular (Hazra et al. (2009)). However, they are least amenable towards *online implementation* owing to the complexities involved in dealing with multiple lagged covariance matrices. Exploiting this impediment, a new online modal identification algorithm is proposed by developing a real-time version of a simple, yet, robust second order statistics based BSS algorithm based on recursive simultaneous diagonalization of covariance matrices (Cichocki and Amari (2002)). The algorithm employs temporal statistics of the responses, projected on an orthogonal space (Cichocki and Amari (2002)) and employs multiple auto-covariance matrices with different lags of the observed multivariate time series.

Recent research in signal processing has focused on statistical theories for vibration mode separation in dynamic systems. Extracting proper orthogonal modes (POMs) aligns with estimating linear normal modes (LNMs) but with some errors (Feeny and Liang (2003)). Algorithms like independent component analysis (ICA) (Hyvärinen and Oja (2000); Yang and Nagarajaiah (2014)) and second-order blind identification (SOBI) have contributed significantly to structural dynamics problems (Parra and Sajda (2003); Hazra et al. (2012)). However, limitations arise due to assumptions of statistical independence and non-Gaussianity in source signals, particularly in highly damped systems, low-energy or closely spaced modes, severe nonstationary excitations, and significant measurement noise (Poncelet et al. (2007); Hazra et al. (2009); Antoni and Chauhan (2013)).

A new class of algorithms – based on first-order eigen perturbation (FOEP) – has emerged as a prominent approach for online modal identification. Recursive canonical correlation analysis (RCCA) (Bhowmik et al. (2022, 2020)) and recursive principal component analysis (RPCA) (Krishnan et al. (2017)) have demonstrated real-time mode separation and damage detection in monitored systems (Krishnan et al. (2018); Bhowmik et al. (2019b)). These approaches are particularly useful when real-time identification of structural faults and their state is challenging. FOEP has also been explored for real-time change detection using a single sensor response (Bhowmik et al. (2019a)). While a semi-adaptive approach to mode separation has been studied by (Amini and Ghasemi (2018)), it implicitly assumes similar conditions as ICA, leaving room for improvements, which are addressed in detail by (Bhowmik et al. (2019b)). Continuous monitoring of working systems aims to detect anomalous events as part

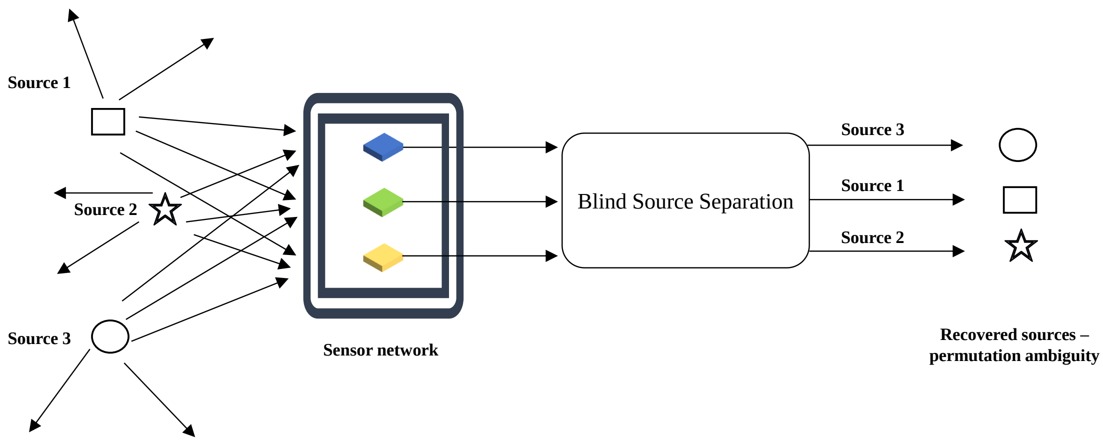

Figure 1: Schematic of BSS methods

of a preventive maintenance policy, leading to energy efficiency benefits, cost savings, and damage prevention. Recursive modal identification algorithms play a key role in this context. Eigenvalue decomposition (EVD) of the covariance matrix formed from response measurements provides the spectral content of the monitored system (Ren and De Roeck (2002)). Variations of EVD, such as generalized eigenvalue decomposition (GEVD), joint diagonalization, unitary factorization, and simultaneous diagonalization of the covariance matrix, have become prominent in recent times Kerschen and Golinval (2002); Feeny and Liang (2003); Zhou and Chelidze (2007). Two classes of algorithms are noteworthy in this regard -

(a) Orthogonalization of basis vectors in a transformed space where the correlation between the physical measurements are minimized (such as principal component analysis (PCA) and its variants (Krishnan et al. (2017, 2018))) and

(b) Affine transformation of physical variables where canonical correlations are invariant, diagonalized and maximized (such as canonical correlation analysis (CCA) and its counterparts (Bhowmik et al. (2022, 2020))). Interpretation of these methods from a broader scope clearly reveal a pattern of source separation, which in turn forms the basis of BSS-based strategies. The basic idea of BSS involves the identification of the parameters of the system based on the knowledge of the outputs. The inputs, referred to as the sources, are usually unknown, which can be mathematically framed as:

$$\left.\begin{aligned} X(k) &= \mathbf{A}S(k) \\ \hat{S}(k) &= \mathbf{W}X(k) \end{aligned}\right\} \tag{1}$$

with $\mathbf{A} = [a_{ij}]_{n\times n}$ being the instantaneous matrix, $\mathbf{W}_{n\times n}$ is the de-mixing matrix to be determined and $\hat{S}$ represents an estimate. As BSS methods seek to determine the de-mixing matrix $\mathbf{W}$ from the information contained in the physical measurements X, the term blind is commonly used. A schematic flow of BSS methods is illustrated in Fig. 1. A recursive setting is used to structure the proposed framework to accommodate online mode separation, impose minimal error convergence, and limit minimum sample population only for algorithm initialization.

This paper introduces a novel approach to blind modal identification by utilizing recursive simultaneous diagonalization based on a generalized eigen perturbation theory. The method presents two optimal *novel* strategies: a) establishing the connection between eigen perturbation and a blind source separation (BSS) framework, and b) utilizing higher-order perturbation theory, known as FOEP, for real-time modal identification and change detection. The proposed approach enables mode separation from streams of response data in the physical domain of vibratory modes, focusing on working infrastructures and providing spectral information in real-time. The **key advantage** of the method lies in its consistent mathematical framework, employing real-time analytics and relieving the need for ad-hoc windowing of data. By enabling simultaneous online updates of vibratory modes and modal responses, the method extends its application to detecting the state of the system, such as transitions between linear and nonlinear regimes. Unlike the joint diagonalization performed using SOBI, the proposed method solves a generalized eigenvalue problem (EVP) through a computationally efficient approach, relying on step-wise eigenspace tracking instead of covariance matrix updates. The paper contributes to the field of blind modal identification by offering a compact and efficient solution that addresses the challenges of real-time analysis and spectral information extraction. The proposed method provides a valuable alternative to existing techniques and showcases the potential for practical implementation in various domains requiring continuous monitoring and detection of system behavior.

The remainder of the paper is structured as follows: *First*, a top-down hierarchy to address blind modal identification in real-time is explored in the backdrop of generalized higher order eigen perturbation approaches. The discussion then focuses on the specialized case of first order eigen perturbation (FOEP) based theoretical investigation, where the structure of the eigenspace is investigated. *Next*, numerically simulated systems are examined in the light of both stationary and non-stationary input excitations for online mode identification. This is followed by a noteworthy discussion on real-time *partial* modal identification for a decentralized network of sensors. A salient performance-based comparison of conventional joint diagonalization approach against the widely-established *ICA* method is reviewed. The simplicity and mathematical convenience of a joint diagonalization approach addresses the shortcomings of a traditional ICA based method - mainly in complete modal recovery in high damping and alleviating the added dependency of maximization of non-Gaussianity. The robustness of the proposed simultaneous diagonalization method is verified using *experimental* test beds conducted in controlled environments. A new *online* condition metric for change of state detection is proposed, which is a real-time transformation of the sought-after Mahalanobis distance. Finally, the applicability of the method in addressing online mode separation for a *practical* system (ASCE-SHM benchmark) is discussed, which concludes the paper.

2. Background

This section consists of two parts. Firstly, the derivation of the first-order eigen perturbation (FOEP) formulation from a generalized higher-order perturbation (HOP) framework is presented. This derivation contributes to the theoretical understanding of the framework and highlights its usefulness in cases where pristine data is unavailable or the anticipation of all possible anomalies is impractical. By exploring the structure of HOP and its sensitivity to eigenvalues, a deeper insight into its relationship with blind source separation (BSS) is gained. The second part focuses on the connection between HOP and BSS within the context of real-time analytics. Given the recursive nature of the framework, the aim is to address the problem of real-time BSS using simultaneous diagonalization techniques. This approach holds significance in engineering applications where continuous monitoring and detection of anomalies are essential, and where the identification of system anomalies in advance is challenging. The exploration of simultaneous diagonalization techniques in the context of real-time analytics enhances the understanding and potential applicability of the proposed framework.

2.1. Recursive covariance estimation in a higher order perturbation framework

A standard form of eigen equation can be derived based on the dynamical behaviour of a system. The discussed approach being an output-only technique, inverse vibration formulations lead to the standard eigen equation as:

$$\mathbf{C}_0\mathbf{V}_0 = \mathbf{\Lambda}_0\mathbf{V}_0 \tag{2}$$

where, $\mathbf{C_0}$ is the covariance matrix composed of the physical responses streamed at the start of monitoring, $\mathbf{V_0}$ and $\mathbf{\Lambda_0}$ are the eigen vector and eigen value matrices – collectively termed as the *eigenspace.*

Consider the rank-n update of the eigenspace that provides the higher eigen perturbation terms. The following definitions for the n^{th} order update of the matrices involved in Eq. 2 will be useful for subsequent derivations:

$$\left.\begin{aligned}\mathbf{C}_n &= \mathbf{C}_0 + \delta\mathbf{C} + \delta^2\mathbf{C} + \delta^3\mathbf{C} + \ldots + \delta^n\mathbf{C}\\ \mathbf{V}_n &= \mathbf{V}_0 + \delta\mathbf{V} + \delta^2\mathbf{V} + \delta^3\mathbf{V} + \ldots + \delta^n\mathbf{V}\\ \mathbf{\Lambda}_n &= \mathbf{\Lambda}_0 + \delta\mathbf{\Lambda} + \delta^2\mathbf{\Lambda} + \delta^3\mathbf{\Lambda} + \ldots + \delta^n\mathbf{\Lambda}\end{aligned}\right\} \tag{3}$$

Substituting the above values in Eq. 2, the n^{th} order update equations can be therefore, formulated as:

$$\begin{aligned}\left(\mathbf{C}_0 + \delta\mathbf{C} + \delta^2 C + \ldots + \delta^n\mathbf{C}\right) = &\left(\mathbf{V}_0 + \delta\mathbf{V} + \delta^2\mathbf{V} + \ldots + \delta^n\mathbf{V}\right)\\ &\left(\Lambda_0 + \delta\Lambda + \delta^2\Lambda + \ldots + \delta^n\Lambda\right)\\ &\left(\Lambda_0 + \delta\Lambda + \delta^2\Lambda + \ldots + \delta^n\Lambda\right)\end{aligned} \tag{4}$$

A detailed expansion of the terms is not provided for brevity. However, the comparison of similar order terms reveal the following equation:

$$\begin{aligned}&\delta^n\mathbf{C} = \mathbf{V}_0\mathbf{\Lambda}_0\delta\mathbf{V}^T + \mathbf{V}_0\delta\mathbf{\Lambda}\delta^{n-1}\mathbf{V}^T + \mathbf{V}_0\delta^2\mathbf{\Lambda}\delta^{n-2}\mathbf{V}^T + \mathbf{V}_0\delta^3\mathbf{\Lambda}\delta^{n-3}\mathbf{V}^T + \ldots\\ &+\mathbf{V}_0\delta^k\mathbf{\Lambda}\delta^{n-k}\mathbf{V}^T + \mathbf{V}_0\delta^n\mathbf{\Lambda}\mathbf{V}_0^T + \delta\mathbf{V}\mathbf{\Lambda}_0\delta^{n-1}\mathbf{V}^T + \delta\mathbf{V}\delta\mathbf{\Lambda}\delta^{n-2}\mathbf{V}^T + \delta\mathbf{V}\delta^2\mathbf{\Lambda}\delta^{n-3}\mathbf{V}^T\\ &+\delta\mathbf{V}\delta^3\mathbf{\Lambda}\delta^{n-4}\mathbf{V}^T + \ldots + \delta\mathbf{V}\delta^k\mathbf{\Lambda}\delta^{n-(k+1)}\mathbf{V}^T + \delta^2\mathbf{V}\mathbf{\Lambda}_0\delta^{n-2}\mathbf{V}^T + \delta^2\mathbf{V}\delta\mathbf{\Lambda}\delta^{n-3}\mathbf{V}^T\\ &+\delta^2\mathbf{V}\delta^2\mathbf{\Lambda}\delta^{n-4}\mathbf{V}^T + \delta^2\mathbf{V}\delta^3\mathbf{\Lambda}\delta^{n-5}\mathbf{V}^T + \ldots + \delta^2\mathbf{V}\delta^k\mathbf{\Lambda}\delta^{n-(k+2)}\mathbf{V}^T + \delta^3\mathbf{V}\mathbf{\Lambda}_0\delta^{n-3}\mathbf{V}^T\\ &+\delta^3\mathbf{V}\delta\mathbf{\Lambda}\delta^{n-4}\mathbf{V}^T + \delta^3\mathbf{V}\delta^2\mathbf{\Lambda}\delta^{n-5}\mathbf{V}^T + \delta^3\mathbf{V}\delta^3\mathbf{\Lambda}\delta^{n-6}\mathbf{V}^T + \ldots + \delta^3\mathbf{V}\delta^k\mathbf{\Lambda}\delta^{n-(k+3)}\mathbf{V}^T\\ &+\delta^n\mathbf{V}\mathbf{\Lambda}_0\mathbf{V}_0^T\end{aligned} \tag{5}$$

A simple expression in terms of discrete summation can be obtained from above:

$$\begin{aligned}&\delta^n\mathbf{C} = \mathbf{V}_0\mathbf{\Lambda}_0\delta\mathbf{V}^T + \mathbf{V}_0\left[\sum_{i=1}^{k}(\delta\mathbf{\Lambda})^i\left(\delta\mathbf{V}^T\right)^{n-i}\right] + \mathbf{V}_0\delta^n\mathbf{\Lambda}\mathbf{V}_0^T + \delta\mathbf{V}\mathbf{\Lambda}_0\delta^{n-1}\mathbf{V}^T +\\ &\delta\mathbf{V}\left[\sum_{i=1}^{k}(\delta\mathbf{\Lambda})^i\left(\delta\mathbf{V}^T\right)^{n-(i+1)}\right] + \delta^2\mathbf{V}\mathbf{\Lambda}_0\delta^{n-2}\mathbf{V}^T + \delta^2\mathbf{V}\left[\sum_{i=1}^{k}(\delta\mathbf{\Lambda})^i\left(\delta\mathbf{V}^T\right)^{n-(i+2)}\right] +\\ &\delta^3\mathbf{V}\mathbf{\Lambda}_0\delta^{n-3}\mathbf{V}^T + \delta^3\mathbf{V}\left[\sum_{i=1}^{k}(\delta\mathbf{\Lambda})^i\left(\delta\mathbf{V}^T\right)^{n-(i+3)}\right] + \delta^n\mathbf{V}\mathbf{\Lambda}_0\mathbf{V}_0^T\end{aligned} \tag{6}$$

The expressions for first order eigen perturbation (FOEP) can be *intuitively* obtained by substituting n=1 in Eq. 6:

$$\delta\mathbf{C} = \mathbf{V}_0\mathbf{\Lambda}_0\delta\mathbf{V}^T + \mathbf{V}_0\delta\mathbf{\Lambda}\mathbf{V}_0^T + \delta\mathbf{V}\mathbf{\Lambda}_0\mathbf{V}_0^T + \mathcal{O}\left(\delta^n\right) \tag{7}$$

For FOEP, perturbation order greater than *one* does not exist (which automatically cancels δ^n terms ($\forall n > 1$), (Bhowmik et al. (2019b))). The cross-matrix multiplication terms are also eliminated in this process - however, spectrally decomposable terms remain intact. An investigation into the perturbation expansion reveals that the expressions obtained above are quite accurate, considering the low magnitude of the perturbation matrices (Stewart (1998)). Distinct eigenvalues initiates the separation of the spectral terms from its neighbors. If this separation ($m-n$ columns of $\mathbf{C}$) is denoted by Δ, then the second order error term is bounded by $\|\delta\mathbf{C}\|^2/\boldsymbol{\Delta}$. In engineering practice $\|\delta\mathbf{C}\|/\boldsymbol{\Delta}$ should be considerably less than one − say one-hundredth and beyond − before one starts to trust this approximation (Bhowmik et al. (2019b)). This result should be treated as a caution for easy rank detection through small singular values. In the presence of noise, singular values tend to proportionately amplify under higher order perturbations (order of $\sqrt{n}$). In practice, this corresponds to acquiring an incorrect rank estimation of the matrices, especially when the sound-to-noise ratio approaches $\sqrt{n}$.

2.2. A note on eigenvalue sensitivity and relation with BSS

An important framework for eigenvalue computation is to produce a sequence of similarity transformations for enforcing strictly diagonally dominant (SDD) matrices. The configuration of these matrices require the investigation of individual elements towards approximating the eigenvalues - i.e., how well do the diagonal elements of the matrix resemble the eigenvalues. This requires consideration of the error norms based on established perturbation theorems which are explained as follows. Throughout this article the notation $\|.\|$ will denote a vector norm when applied to a vector and an operator matrix norm when applied to a matrix.

Theorem 1: *Gershgorin's Circle Theorem.*

Let $\mathbf{A}$ be an arbitrary $n\times n$ matrix with λ as any one of the eigenvalues of $\mathbf{A}+\mathbf{E}$, where $\mathbf{E}$ is a small perturbation with zero diagonal entries. The spectral decomposition of the matrix can be expressed as:

$$\mathbf{A}+\mathbf{E}=\mathbf{V}\boldsymbol{\Lambda}\mathbf{V}^{-1} \tag{8}$$

The mathematical identity using Gershgorin theorem provides the equation:

$$\lambda\left(\boldsymbol{\Lambda}\right)\subseteq\bigcup_{i=1}^{n}\mathbf{A}_i \tag{9}$$

where, $\mathbf{A}_i=\left\{z\in\Re:|z-a_i|\leq\sum_{j=1}^{n}|e_{ij}|\right\}$

Proof:

Without loss of generality, suppose $\lambda\in\lambda\left(\boldsymbol{\Lambda}\right)$ for which $\lambda\neq a_i\ \forall i=1:n$. As $(\mathbf{A}-\lambda\mathbf{I})+\mathbf{E}$ is singular, it follows from Lemma 1 (**Appendix A**) that:

$$1\leq\left\|\left(\mathbf{A}-\lambda\mathbf{I}\right)^{-1}\mathbf{E}\right\|_{\infty}=\sum_{j=1}^{n}\frac{|e_{kj}|}{|a_k-\lambda|} \tag{10}$$

$\forall k=1:n$. However, this implies that $\lambda\in\mathbf{A}_k$. The proof establishes that the diagonal portion of the covariance matrix so obtained approximates the eigenvalue of the matrix. It follows that the *matrix* *bears an SDD structure*, which enables recursive updates of the eigenspace at each instant. This forms the key cornerstone of FOEP analyses that enables online recovery of structural modes from a dynamic system.

Theorem 2: *Bauer-Fike Theorem.*

Although the Bauer-Fike theorem discusses eigenvalue perturbation of diagonalizable matrices (which are mostly SDD), it essentially studies the localization of eigenvalues that are concentrated within small regions of the complex plane. This theorem can be considered as a generalization of the Gershgorin's circle theorem – but for the purposes of this article, discussions are limited to operator norms, derived from related vector norms.

Theorem: Let $\mathbf{A}$ be an arbitrary $n \times n$ diagonalizable matrix satisfying $\mathbf{A} = \mathbf{V}\boldsymbol{\Lambda}\mathbf{V}^{-1}$ and let $\mathbf{E}$ be a small perturbation matrix. Every eigenvalue μ of the matrix $\mathbf{A} + \mathbf{E}$ satisfies:

$$\min_{\lambda \in \lambda(A)} |\mu - \lambda| \leq \|\mathbf{V}\| \,.\, \left\|\mathbf{V}^{-1}\right\| \,.\, \|\mathbf{E}\| \tag{11}$$

where λ is some eigenvalue of $\mathbf{A}$.

Proof:

A straightforward explanation of the theorem would suggest its veracity if $\lambda \in \lambda(\boldsymbol{\Lambda})$. Contrary to this idea, considering the singularity of $\mathbf{V}^{-1}(\mathbf{A} + \mathbf{E} - \lambda\mathbf{I})\,\mathbf{V}$, $\mathbf{I} + (\mathbf{A} - \lambda\mathbf{I})^{-1}\left(\mathbf{V}^{-1}\mathbf{E}\mathbf{V}\right)$ also becomes singular. From Lemma 1, the following inequality is obtained:

$$1 \leq \left\|(\mathbf{A} - \lambda\mathbf{I})^{-1}\left(\mathbf{V}^{-1}\mathbf{E}\mathbf{V}\right)\right\|_p \leq \left\|(\mathbf{A} - \lambda\mathbf{I})^{-1}\right\|_p \|\mathbf{X}\|_p \|\mathbf{E}\|_p \left\|\mathbf{X}^{-1}\right\|_p \tag{12}$$

As $(\mathbf{A} - \lambda\mathbf{I})^{-1}$ is diagonal and the p-norm of a diagonal matrix automatically translates to the absolute value of the largest diagonal entry, it follows that

$$\left\|(\mathbf{A} - \lambda\mathbf{I})^{-1}\right\|_p = \min_{\lambda \in \lambda(A)} \frac{1}{|\mu - \lambda|} \tag{13}$$

which completes the proof. If $\|\mathbf{E}\|$ is small, then the theorem states that the eigenvalues of $\mathbf{A} + \mathbf{E}$ are close to that of $\mathbf{A}$. Interestingly, the distance between the eigenvalues of $\mathbf{A} + \mathbf{E}$ and $\mathbf{A}$ vary linearly with the perturbation matrix $\mathbf{E}$, which forms yet another fundamental hypothesis of eigen perturbation theory.

Certain cases require the perturbation bounds to be computed on singular vectors. Since the individual singular vectors corresponding to a cluster of singular values is unstable, bounds for the subspace spanned by the singular vectors – known as the *singular subspace* – are computed. For two one dimensional subspaces $\mathcal{X}$ and $\mathcal{Y}$, the angle between the subspaces is given by: $\theta = \cos^{-1}\left|x^T y\right|$, where x and y are the vectors of norm one spanning $\mathcal{X}$ and $\mathcal{Y}$. In a more generalized sense, for complex dynamical systems, this construction can be expanded to subspaces of dimension k. Considering x and Y to be the orthonormal bases for $\mathcal{X}$ and $\mathcal{Y}$ respectively, the above expression can be formulated as:

$$\theta_i|_k = \cos^{-1}|\gamma_i|_k \tag{14}$$

where, $\gamma_1 \geq \gamma_2 \geq \ldots \geq \gamma_i$ are the singular values of $X^T Y$. The formulated measure is then referred to as *canonical angle* that provide a distance metric between the subspaces. An important step in identifying modal structure from output responses involves projecting a source p to a 1D orthogonal space (pre-whitening step) where the p^{th} component resides. It is therefore, worthwhile to note the connection between canonical angles and projections. Consider P_X and P_Y to be the orthogonal projections onto $\mathcal{X}$ and $\mathcal{Y}$. If $\mathcal{X}$ and $\mathcal{Y}$ are equal, it naturally follows that $P_X = P_Y$, which retains $\|P_X = P_Y\|$ as the distance metric. However, for a generalized treatment of the random subspaces, it can be shown that the Frobenius norm is related to the canonical projection as:

$$\|P_X = P_Y\|_F = \sqrt{2}\|\sin\theta\|_F \tag{15}$$

Thus the two measures decay to zero at the same rate. This allows for the systematic manifestation of orthonormal projections that form the preliminary step of the recursion algorithm.

3. Problem formulation

Given a series of observed signals, BSS aims at recovering the underlying sources embedded in measured data by assuming temporal correlation. Mathematically, the BSS model can be written as $X = \mathbf{A}Z$, with an unknown full rank $p \times p$ mixing matrix $\mathbf{A}$, and the aim, based on the observations $x_1, x_2, \ldots, x_n$, is to find an estimate of $\mathbf{A}$ (or its inverse), such that $\mathbf{A}^{-1}X$ recover the sources Z. In real applications, temporal and spatial dependence between the observations should be incorporated, which modifies the model to: $X(t) = \mathbf{A}Z(t)\ \forall\ t \in \mathcal{R}^{p\times 1}$, where Z is a p-variate time series that satisfies (Zhou and Chelidze (2007)):

- $E(Z(t)) = 0$
- $E(Z(t), Z'(t)) = \mathbf{I}_p$
- $E(Z(t), Z'(t+\tau)) = \mathbf{D}_p,\ \forall\ \tau = 1, 2, \ldots$,n

Consider the governing equations of motion for a multi degree-of-freedom (DOF) linear vibrating system under the action of an excitation force vector $F(t)$:

$$\mathbf{M}\ddot{X}(t) + \mathbf{C}\dot{X}(t) + \mathbf{K}X(t) = F(t) \tag{16}$$

where $X(t)$ is the vector of displacement. Assuming the output signals are sampled at Δt time period for a total of p recorded data points, the structural responses in the physical and modal domain are related as: $\mathbf{X} = \mathbf{W\Phi}$, where $\mathbf{X} \in \mathcal{R}^{p\times p}$ is the matrix of physical responses, $\mathbf{W}$ is the mode shape matrix and $\mathbf{\Phi}$ is the matrix of corresponding modal coordinates. The algorithm assumes that: (**1**) The mixing matrix $\mathbf{A}$ is of full column rank. (**2**) Sources are spatially uncorrelated with different autocorrelation functions but temporally correlated stochastic signals with zero mean. (**3**) Variance of sources are time-varying. The preliminary structure of the block covariance matrix is given by:

$$\mathbf{Cov}\left(\begin{array}{c} X_t \\ X_{t+\tau} \end{array} \right)\Bigg|_k = \begin{bmatrix} \mathbf{R}_{X,k} & \hat{\mathbf{R}}_{X,k} \\ \hat{\mathbf{R}}^T_{X,k} & \mathbf{R}_{X,k} \end{bmatrix} \tag{17}$$

The primary step for the recursive diagonalization algorithm is to perform an *online pre-whitening* which is an FOEP-based RPCA approach (Krishnan et al. (2018)). The covariance estimate of the physical responses can be expressed as:

$$\mathbf{R}_X(k) = \frac{k-1}{k}\mathbf{\Sigma}_k^{-1}\mathbf{\Sigma}_{k-1}\mathbf{R}_X(k-1)\mathbf{\Sigma}_{k-1}\mathbf{\Sigma}_k^{-1} + \mathbf{\Sigma}_k^{-1}\Delta\mu_k\Delta\mu_k^T\mathbf{\Sigma}_k^{-1} + \frac{1}{k}\left[X_k - \mu_k\right]\left[X_k - \mu_k\right]^T \tag{18}$$

Post-whitening, the eigenspace updates at the k^{th} instant can therefore, be obtained as: $\mathbf{W}_k = \mathbf{W}_{k-1}\mathbf{H}_k$ *and* $\gamma_k = \frac{\mathbf{\Gamma}_k}{k}$. Here, μ_k and $\mathbf{\Sigma}_k$ are the mean and standard deviation of the i^{th} measured variable ($i = 1, ..., p$) and $\mathbf{H}_k$, $\mathbf{\Gamma}_k$ are the decomposed spectral components of the diagonally dominant eigenspace at the k^{th} instant. The whitened signal matrix becomes:

$$Z(k) = \gamma_k^{-1/2}\mathbf{W}_k^T X_k \tag{19}$$

where, γ and $\mathbf{W}$ correspond to the eigenvalue and eigenvector matrices, respectively. Covariance matrix of transformed response for non-zero lag (τ=1) is given by:

$$\begin{aligned} \hat{\mathbf{R}}^T_{Z,k} = \tfrac{1}{2}\left[\mathbf{R}_{Z,k} + \mathbf{R}^T_{Z,k}\right] &= \tfrac{1}{2}\gamma_k^{-1/2}\mathbf{W}_k^T\left[X_k X_{k,\tau}^T + X_{k,\tau}X_k^T\right]\mathbf{W}_k\gamma_k^{-1/2} \\ &= \gamma_k^{-1/2}\mathbf{W}_k^T\hat{\mathbf{R}}_{x,k}\mathbf{W}_k\gamma_k^{-1/2} \end{aligned} \tag{20}$$

where, $\hat{\mathbf{R}}_X(k) = \frac{1}{2}\left[X_k X_{k,\tau}^T + X_{k,\tau}X_k^T\right]$. Substituting the EVD of the covariance matrix ($\mathbf{R}_Z(k) = \mathbf{U}_Z(k)\mathbf{\Lambda}_Z(k)\mathbf{U}_Z^T(k)$) in the above expression and post-multiplying both sides by $\gamma_k^{-1/2}\mathbf{W}_k^T$, one obtains:

$$\begin{aligned} &\gamma_k^{-1/2}\mathbf{W}_k^T\left[\tfrac{k-1}{k}\mathbf{\Sigma}_{k,\tau}^{-1}\mathbf{\Sigma}_{k-1,\tau}\mathbf{R}_{X,\tau}(k-1)\mathbf{\Sigma}_{k-1,\tau}\mathbf{\Sigma}_{k,\tau}^{-1} + \mathbf{\Sigma}_{k,\tau}^{-1}\Delta\mu_{k,\tau}\Delta\mu_{k,\tau}^T\mathbf{\Sigma}_{k,\tau}^{-1} + \right. \\ &\left.\tfrac{1}{k}\left[X_{k,\tau} - \mu_{k,\tau}\right]\left[X_{k,\tau} - \mu_{k,\tau}\right]^T\right]\mathbf{W}_k\gamma_k^{-1}\mathbf{W}_k^T = \mathbf{U}_Z(k)\mathbf{\Lambda}_Z(k)\mathbf{U}_Z^T(k)\gamma_k^{-1/2}\mathbf{W}_k^T \end{aligned} \tag{21}$$

Pre-multiplying both sides by $\mathbf{U}_Z^T(k)$, scaling the signal to unit variance and considering a zero-mean process (usual for structural dynamics applications):

$$\begin{aligned}&\mathbf{U}_Z^T(k)\gamma_k^{-1/2}\mathbf{W}_k^T\left[\tfrac{k-1}{k}\mathbf{R}_{X,\tau}(k-1)+\tfrac{1}{k}\left[X_{k,\tau}-\mu_{k,\tau}\right]\left[X_{k,\tau}-\mu_{k,\tau}\right]^T\right]\mathbf{W}_k\gamma_k^{-1}\mathbf{W}_k^T\\&=\mathbf{\Lambda}_Z(k)\mathbf{U}_Z^T(k)\gamma_k^{-1/2}\mathbf{W}_k^T\end{aligned}\tag{22}$$

Substituting $\psi_k^T=\mathbf{U}_Z^T(k)\gamma_k^{-1/2}\mathbf{W}_k^T$ and noticing that $\mathbf{W}_k\gamma_k^{-1}\mathbf{W}_k^T=\mathbf{R}_X^{-1}(k)$, Eq. 22 becomes:

$$\psi_k^T\hat{\mathbf{R}}_X(k)=\mathbf{\Lambda}_{Z,k}\psi_k^T\mathbf{R}_X(k)\tag{23}$$

ψ_k is the generalized eigenvector matrix. At this stage, it can be very well understood that Eq. 23 needs to be recursively updated for each sample. For this, consider the rank-one perturbation of the eigen decomposition given by Eq. 23:

$$\left(\psi_k^T+\Delta\psi_k^T\right)\left(\hat{\mathbf{R}}_{X,k}+\Delta\hat{\mathbf{R}}_{X,k}\right)=\left(\mathbf{\Lambda}_{Z,k}+\Delta\mathbf{\Lambda}_{Z,k}\right)\left(\psi_k^T+\Delta\psi_k^T\right)\left(\mathbf{R}_{X,k}+\Delta\mathbf{R}_{X,k}\right)\tag{24}$$

Reiterating the central concept of FOEP that essentially involves the updates of eigenspace without actually performing stepwise EVD on covariance matrices, the term-wise expansion of the above equation yield:

$$\psi_{k+1}^T=\mathbf{\Lambda}_{Z,k+1}\hat{\mathbf{R}}_X^{-1}(k+1)\psi_{k+1}^T\mathbf{R}_X(k+1)\tag{25}$$

To obtain the eigenspace at each time stamp, Eq. 24 needs to be recursively solved that involves solving the generalized eigen value problem through matrix inversion. Resorting to Woodbury's identity (that can provide the inverse of any full rank matrix), the solution to Eq. 25 is as follows:

$$\begin{aligned}\hat{\mathbf{R}}_X(k+1)&=\tfrac{k}{k+1}\hat{\mathbf{R}}_{X,k}+\tfrac{1}{k+1}\begin{bmatrix}0&\hat{X}_k\hat{X}_{k,\tau}^T\\\hat{X}_{k,\tau}\hat{X}_k^T&0\end{bmatrix}\\&=\mathbf{P}+\mathbf{QU}\end{aligned}\tag{26}$$

where the product $\mathbf{QU}$ is given by:

$$\mathbf{QU}=\frac{1}{k+1}\begin{bmatrix}0&\hat{X}_k\\\hat{X}_{k,\tau}&0\end{bmatrix}\begin{bmatrix}\hat{X}_{k,\tau}^T&0\\0&\hat{X}_{k,\tau}^T\end{bmatrix}\tag{27}$$

Using Woodbury's identity, the inverse of the matrix $\hat{\mathbf{R}}_X(k+1)$ can now be computed as:

$$\begin{aligned}\hat{\mathbf{R}}_X^{-1}(k+1)&=\left[\mathbf{P}(k+1)+\mathbf{Q}(k+1)\mathbf{U}(k+1)\right]^{-1}\\&=\mathbf{P}^{-1}(k+1)-\mathbf{P}^{-1}(k+1)\mathbf{Q}(k+1)*\\&\left[\mathbf{U}^{-1}(k+1)+\mathbf{P}^{-1}(k+1)\mathbf{Q}(k+1)\right]^{-1}\mathbf{P}^{-1}(k+1)\end{aligned}\tag{28}$$

Simplifying and carrying out appropriate substitutions, the de-mixing matrix can be obtained as:

$$\psi_k^{-T} = \hat{\mathbf{A}}(k) = \mathbf{W}_k \gamma_k^{1/2} \mathbf{U}_Z(k) \tag{29}$$

The symmetry of the cross-covariance matrix $\hat{\mathbf{R}}_X(k)$ is associated with the number of dimensions for the reconstructed signal matrix at the k^{th} instant. In case $\hat{\mathbf{R}}_X(k)$ is asymmetric, not only the extracted mixing modes complex, but the desired diagonalization needs to be carried out using both right and left generalized eigenvector matrices.

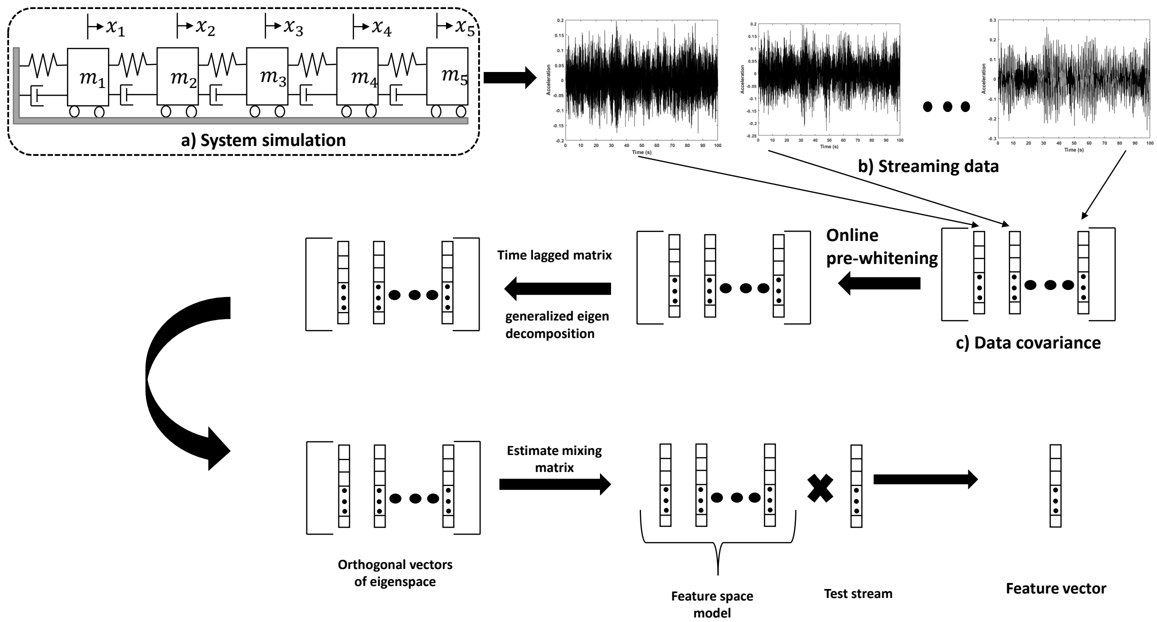

Figure 2: Schematic of recursive modal identification process

4. Algorithm methodology

Most anomaly detection methods in the field assume cost insensitivity, treating misclassification errors and anomalous points as equally costly without considering the different risks they pose. This limitation affects the performance of traditional algorithms in correctly classifying faults based on their occurrence. Hence, the real-time identification of a system's dynamical state becomes crucial. This work addresses the issue of change detection as a decision-making process. The proposed method starts by utilizing data streams and constructing covariance matrices from the physical response obtained through a sensor network. Unlike traditional approaches, the framework avoids real-time diagonalization of multi-lagged covariance matrices and instead incorporates two auto-covariance matrices with different lags. The modal identification module is then employed, performing eigenspace updates at each sample point. The accuracy of the estimated linear normal modes (LNMs) is assessed by comparing them with their theoretical counterparts. Once the recursive estimation of modes begins, a real-time distance measure, such as the recursive Mahalanobis distance (RMD), is used to monitor the transition of the system's regime between linear and nonlinear states. Visual analysis of the distance measures reveals the evolution of state changes. An easy comprehension of the methodology is enumerated as follows:

1. First, covariance matrices of the physical responses at time lags 0 and $\tau = 1$ are evaluated. Simultaneous diagonalization of these matrices are carried out in an offline mode for initial number of samples (around 100 in number) in order to estimate the initial eigenspace. The choice of sample size here is based on the stabilization of the algorithm. The selected number of samples corresponds to a specific duration of time, and it aligns with the temporal granularity required for an accurate representation of the behavior of the system. The computational steps that follow the offline initialization are designed to adapt in real-time to changes in the behavior of the system.

2. With an online pre-whitening technique, the mixed signal is transformed to a space where the correlations between the physical responses are minimized.

3. Recursive eigenspace estimation of the time-lagged covariance matrix is then carried out to produce orthogonal basis vectors.

4. Using a generalized eigen inversion-decomposition, the de-mixing matrix is recursively obtained at each sample point. This step simultaneously yields the feature vectors which correspond to the LNMs of the monitored system. These are then compared against the theoretical modes and the modal assurance criteria (MAC) is recursively evaluated to indicate the correctness of fit.

5. Once the modes are recursively obtained, the system is investigated for any change of state. Distance measures such as the RMD is plotted corresponding to the transformed responses obtained at Step 4. Significant distortions indicating a change of trend or deviation of mean level indicate the transition of state for the system.

Additionally, the schematics of the recursive modal identification approach is illustrated in Fig. 2.

5. Numerical studies

The deficiencies of traditional BSS algorithms and motivation for the proposed approach based on recursive diagonalization is highlighted by considering the following numerically simulated systems: (a) *a 5-DOF linear system*, investigated for both *complete* and *partial* mode recovery and (b) a 3-DOF *test* linear system – especially designed to demonstrate the efficacy of joint diagonalization over the conventional ICA method.

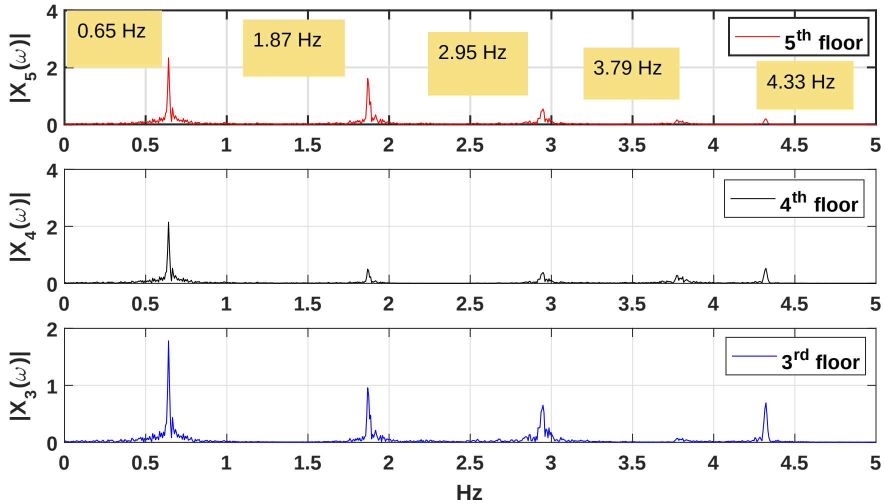

Figure 3: Spectral representation of vibratory modes for the 5 DOF system

5.1. 5 DOF system: Description and investigation

A noisy environment is used to assess the effectiveness of the proposed technique in a simulated study of a 5-degree-of-freedom (DOF) vibrating system. The system consists of floors with a mass of $10kg$ each and individual stiffness of $2kN/m$. The damping ratio for each mode is set at $\zeta = 2.0\%$ critical for each mode. The simulation is conducted with a sampling interval of 100 Hz over a duration of 100s using synthetic Gaussian stationary white noise with zero mean and unit variance, along with additive noise. All DOFs of the system are instrumented, and the complete set of physical responses is utilized. Fig. 3 illustrates a typical frequency domain representation of the system response, displaying modal peaks at frequencies of 0.65, 1.87, 2.95, 3.79 and 4.33 Hz, respectively. The correlation between the theoretical modes and the estimated linear normal modes (LNMs) obtained through recursive simultaneous diagonalization is evaluated using Modal Assurance Criterion (MAC) values, as defined in (defined in Eq. 30). As the modal identification is performed in real-time, a departure from the conventional approach is made by obtaining a vector of MAC values corresponding to each sample point, rather than a single MAC value for each mode. The estimated mode shapes are expected to converge to the theoretical modes over time. This setup enables the assessment of the proposed technique's performance in a noisy environment, providing insights into the convergence of estimated mode shapes to their theoretical counterparts as the system evolves in time. The expression to obtain MAC values in real-time is shown as follows:

$$\mathrm{Rec} - MAC_{i,k} = \frac{\left(\phi_{i,k}^T \varphi_{i,k}\right)^2}{\left(\phi_{i,k}^T \phi_{i,k}\right)\left(\varphi_{i,k}^T \varphi_{i,k}\right)} \tag{30}$$

Here $\phi_{i,k}$ and $\varphi_{i,k}$ represent the i^{th} theoretical and estimated mode shape vectors, respectively corresponding to the k^{th} sample. The convergence of modal recovery is assessed using the Modal Assurance

Criterion (MAC) value, with complete recovery achieved when the MAC value reaches unity. In this recursive approach, the convergence is measured over time in terms of sample evolution. Results from the study indicate that approximately 20% of the sample size is required initially to stabilize the recursion before observing convergence.

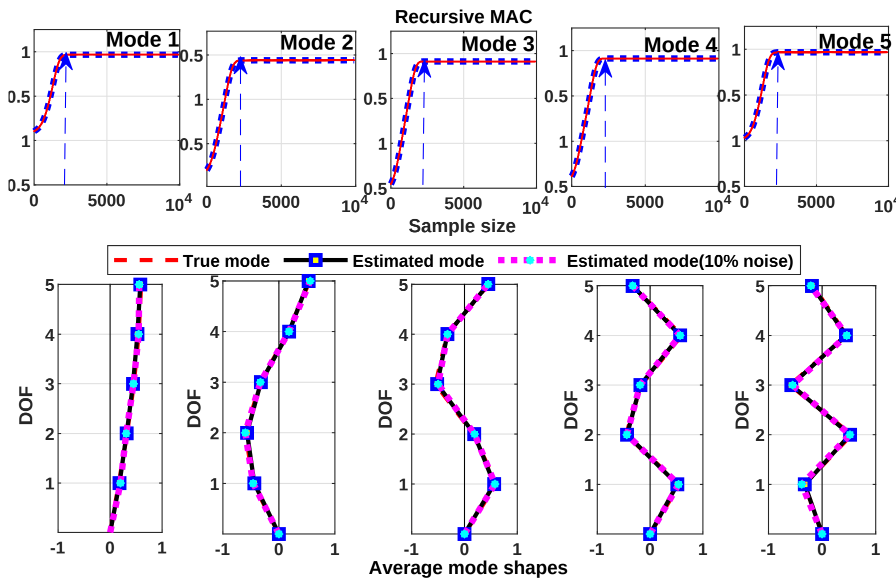

Figure 4: Recursive evolution of MAC across samples for linear 5DOF system under white noise excitation

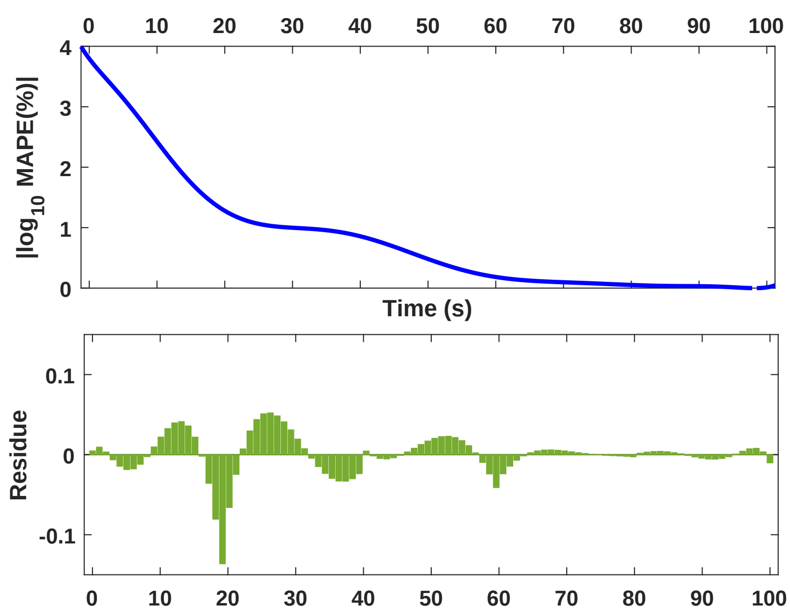

Figure 5: MAPE and residual error plots for eigenspace updates

A short description of the methodology is provided: First, the streaming output response is structured to provide initial covariance estimate for 100 samples. Using FOEP, the eigenspace updates at subsequent samples are obtained, leading to step-wise estimation of the system's spectral content. The generated LNMs in turn are compared against the theoretical modes of the system and the corresponding MAC values are plotted in recursion. The plots in Fig.4 clearly indicate that: **(a)** the recursive MAC values start converging to unity at about 20% of the sample size – indicating near-perfect correlation – which remains invariant across subsequent samples, and **(b)** the average modes estimated using recursive diagonalization is in close agreement with the theoretical mode shapes. With an error estimate of less than *1%* even for cases with *10%* additive noise, the proposed method is therefore, effective in recursively evaluating vibrating modes in real-time.

The accuracy of the observed eigenspace can be assessed through the development of an *error metric* that performs in real-time, known as the recursive maximum absolute percentage error (re-MAPE) (Mucchielli et al. (2020)). To establish this metric, the POM corresponding to each sample point is compared against the theoretical LNM for the vibrating system. With $\mathbf{\Phi}_{theo}$ as the theoretical mode shape matrix and $\mathbf{\Phi}_{i,k}$ as the eigenvector obtained at each instant i corresponding to the k^{th} sample, one can obtain the recursive error metric is expressed as:

$$re - MAPE = \frac{1}{n^2} \sum_{i=1}^{n} \sum_{k=1}^{n} \left(\left| \frac{\mathbf{\Phi}_{theo} - \mathbf{\Phi}_{i,k}}{\mathbf{\Phi}_{theo}} \right| \right) \tag{31}$$

The error plot in Fig. 5 demonstrates that the error percentage asymptotically converges as the sample population increases. The graph attenuation observed from 20 seconds onwards supports the claim of a 20% convergence rate for recursive MAC values. This finding is particularly relevant for remote monitoring applications where the measurement stream may be affected by various factors (such as sensor malfunctioning, erratic power source or unreliable weather), and only short monitoring periods are feasible. The residual plot in Fig. 5 provides a sample-wise tracking of the metric, indicating that an imaginary envelope enclosing the plot would show perfect attenuation from 20 seconds. The steady progression of the residues towards minimal values further confirms the reliability of this framework for real-time modal identification.

In the context of SHM, an effective system should be capable of detecting structural damage at an early stage and providing valuable information for post-event damage assessment. When a structure is subjected to non-stationary excitation, such as earthquake ground motion, achieving complete modal recovery is more challenging compared to free vibrations. Additionally, the time-varying nature of structural properties prevents the implementation of classical Fourier-based deconvolution methods for extracting the impulse response from the output vibration. Given that the energy of the vibration response is concentrated in frequency bands corresponding to the system's natural frequencies, it is worth investigating the performance of recursive modal extraction using the proposed algorithm. In this study, a Kanai-Tajimi (K-T) stochastic model is considered, which accounts for time-dependent frequency and amplitude modulation (Rofooei et al. (2001)). The simulated ground motion, with a normalized peak response duration of 0.4, has a dominant earthquake excitation frequency of 3.5 Hz and lasts for 30 seconds. From Fig.6 it can be observed that the MAC values converge towards unity at around 20-22% of the sample size, which is significant considering the limited duration of output responses typically obtained from field studies. Moreover, the average LNMs obtained across samples remain consistent, except for higher modes of lesser significance. These findings establish the effectiveness of the proposed method for modal identification in practical scenarios, such as earthquake events.

$$\left.\begin{aligned} \ddot{X}_f + 2\eta_g(t)\omega_g(t)\dot{X}_f + \omega_g^2(t)X_f &= W_n(t) \\ \ddot{X}_g &= -a_e(t)(2\eta_g(t)\omega_g(t)\dot{X}_f + \omega_g^2(t)X_f) \end{aligned}\right\} \tag{32}$$

Here, X_f is the filtered response, $\omega_g(t)$ is the time dependent ground frequency, $\eta_g(t)$ is the effective ground damping coefficient, $a_e(t)$ is the amplitude envelop function and $\ddot{X}_g$ is the output ground acceleration.

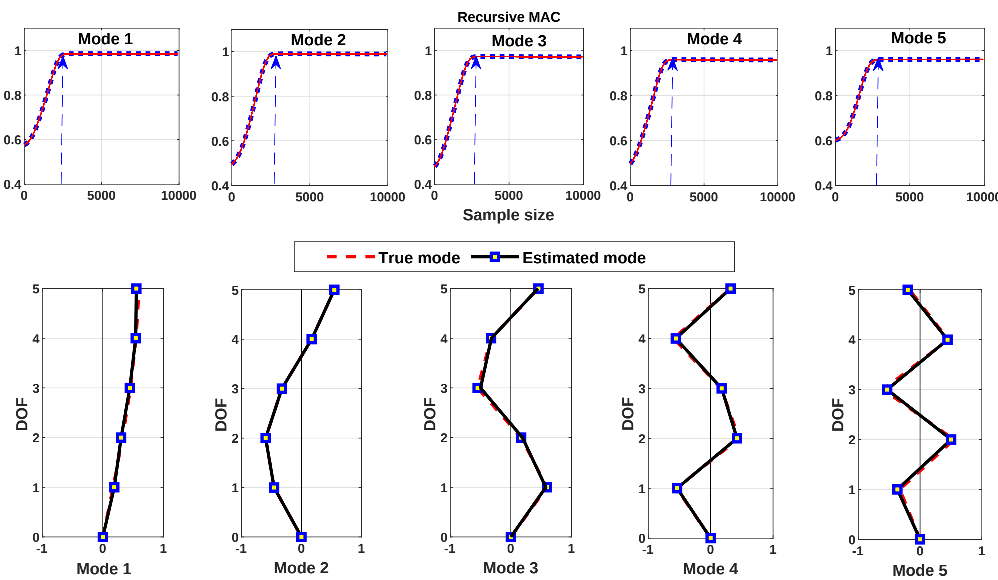

Figure 6: Recursive evolution of MAC across samples for linear 5DOF system under non-stationary excitation

5.2. Partial real-time modal identification : Description and investigation

Conventional modal identification algorithms typically involve offline processing of output measurements collected from multiple sensors, known as centralized implementation. However, practical considerations such as monitoring cost, accessibility constraints, and sensor availability may require the instrumentation of selected DOFs that capture the most significant system dynamics (from an algorithmic viewpoint, this should be equal to the number of principal components explaining more than 90% of variance) (Bhowmik et al. (2019a))). This approach – known as *decentralized implementation* or*underdetermined identification* – allows information extraction from a subset of sensors for health monitoring purposes (Gao et al. (2006); Zimmerman et al. (2008)). In a decentralized framework, the challenge lies in dealing with an underdetermined set of equations when the number of measurement channels is fewer than the actual DOFs. From a BSS standpoint, the challenge in a decentralized

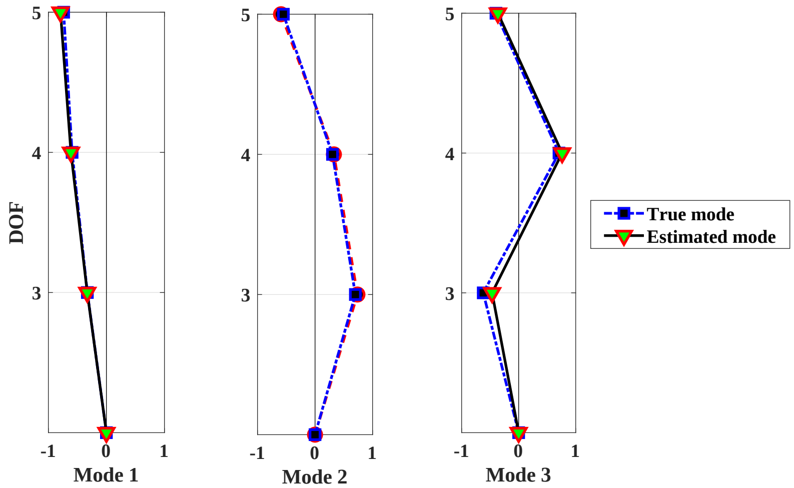

Figure 7: Partial (underdetermined) real-time modal identification for the 5-DOF system

framework leads to an underdetermined set of equations (where the number of measurement channels is less than the actual DOF) that becomes more involved if attempted in a real-time framework.

To assess the applicability of the proposed method in situations where only a subset of sensor information is available, a simulated 5 DOF system was considered. The response was streamed from sensors placed on the 3^{rd}, 4^{th} and 5^{th} floors. The response obtained from this subset of sensors was used to form a partial covariance matrix, which was recursively pre-whitened. The transformed responses at each time stamp were used to simultaneously update the eigenspace characteristics, resulting in the estimation of mode shapes for each sample point. An ensemble average of the estimated modes are plotted against the LNMs of the system in Fig. 7. The figure demonstrates a near-perfect correlation between the estimated modes and the true modes, highlighting the robustness of the proposed method for real-time modal identification using a partial set of sensors. The proposed decentralized implementation approach addresses the challenge of underdetermined identification and extends the applicability of the method to scenarios where limited sensor information is available. This capability is crucial for practical situations with cost and accessibility constraints, and it showcases the effectiveness of the proposed method for real-time modal identification.

To ensure meaningful data extraction from sensors, it is crucial to recommend fault-related features that are highly relevant, minimally redundant, and strongly correlated with the fault. The findings of this study support the utilization of blind recursive simultaneous diagonalization as a basis for developing a framework with potential applications in real-time decentralized/wireless SHM. Although this study did not specifically explore these applications, there is significant value in developing algorithms that address partial modal identification with a permanently instrumented DOF (*permanent* at least for the monitored duration) and a mobile set of sensors providing intermittent subsets of information from locally monitored floor levels. In such scenarios, it is important to consider the possibility of mode mixing, which can be mitigated using the recursive singular spectrum analysis (RSSA) algo-

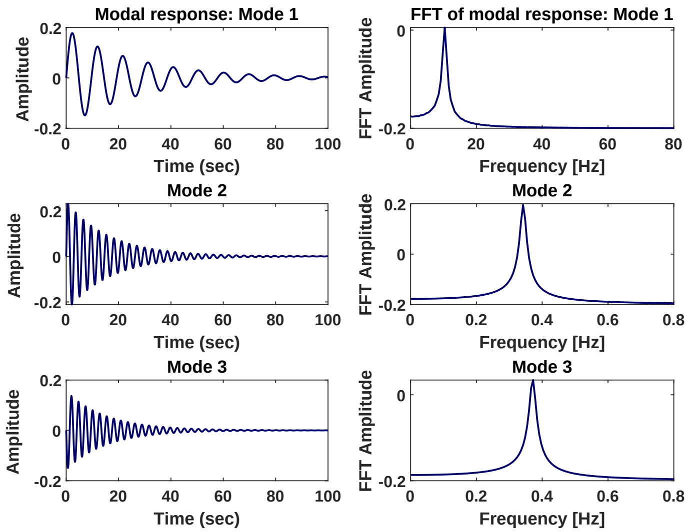

Figure 8: Modal response of the 3DOF system

rithm based on the framework of FOEP (Bhowmik et al. (2019a)). RSSA offers a computationally efficient online filtering technique that can effectively handle mode mixing. Further details on the RSSA algorithm can be found in Bhowmik et al. (2019a). The development of algorithms for partial modal identification with a combination of permanent and mobile sensors has significant implications for real-time decentralized and wireless SHM. By leveraging blind recursive simultaneous diagonalization and incorporating techniques like RSSA, it is possible to advance the field of SHM and enable effective monitoring and fault detection in structures with a dynamic sensor configuration.

5.3. Test problem for a comparative investigation

In real-world problems, the presence of unregulated structural damping poses challenges to accurate modal identification. Damping, which is primarily influenced by material properties, can be categorized into light damping (less than 2% in each mode), moderate damping (2-5%), and high damping (beyond 5%). It has been observed that high damping levels significantly hinder complete modal recovery. Therefore, the performance of the traditional blind source separation (BSS) based joint diagonalization algorithm is investigated in the context of high modal damping. The aim of this investigation is to evaluate the effectiveness of the proposed method in comparison to a well-established technique such as independent component analysis (ICA). The simulated 3 DOF system under consideration is found in the work of McNeill and Zimmerman (2008); the structural properties of which are provided as under:

$$\mathbf{M} = \begin{bmatrix} 1 & 0 & 0 \\ 0 & 2 & 0 \\ 0 & 0 & 1 \end{bmatrix}, \mathbf{K} = \begin{bmatrix} 5 & -1 & 0 \\ -1 & 4 & -3 \\ 0 & -3 & 3.5 \end{bmatrix} \text{ and } \mathbf{C} = \begin{bmatrix} 0.0894 & -0.0084 & 0.0003 \\ -0.0084 & 0.1301 & -0.0244 \\ 0.0003 & -0.0244 & 0.0772 \end{bmatrix}$$

Free decay from initial conditions was considered for simulation. The modal displacement obtained analytically are shown in Fig. 8. Notice that modes 2 and 3 are fairly closely spaced.

The initial application of independent component analysis (ICA) for mode separation – as shown in Fig. 9 –eveals that closely spaced modes are not effectively separated, resulting in components with amplitude modulation. To assess the accuracy of the estimated mode shapes compared to the theoretical ones, the MAC metric is used here. The MAC results obtained using ICA, as presented in Table 1, demonstrate a high correlation close to unity. However, this fails to demonstrate the effectiveness of ICA in separating closely spaced modes in the presence of high damping.

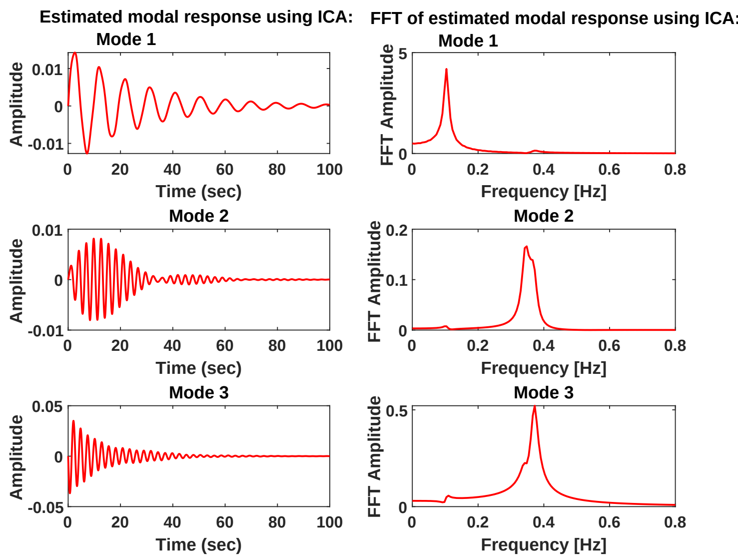

Figure 9: Estimated modal responses using ICA

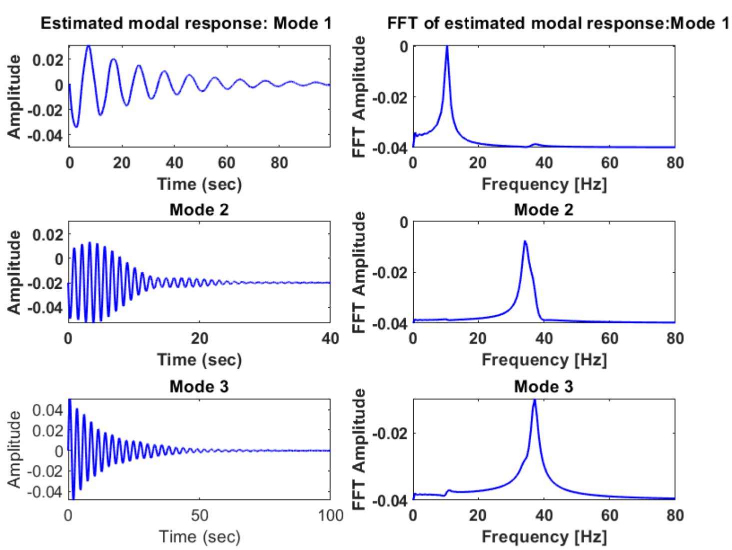

Figure 10: Estimated modal responses using joint diagonalization

In contrast, the proposed approach employs simultaneous diagonalization at each lag, ensuring accurate mode extraction for the system. Despite being imperfect, the mode extraction using this method outperforms ICA, especially in the presence of high modal damping. Table 1 clearly shows a significant correlation close to unity in the column containing the MAC values, indicating that joint diagonalization of covariance matrices at each lag enables effective separation of closely spaced modes even under high damping conditions.

Table 1: Estimated natural frequency and MAC values

Mode no.	Analytical		ICA		Joint diagonalization	
	Frequency (Hz)	Correlation	Frequency (Hz)	MAC-ICA	Frequency (Hz)	MAC-joint diag.
1	0.104	1.0000	0.105	0.9899	0.104	1.0000
2	0.343	1.0000	0.348	0.9797	0.347	0.9986
3	0.371	1.0000	0.373	0.9873	0.372	1.0000

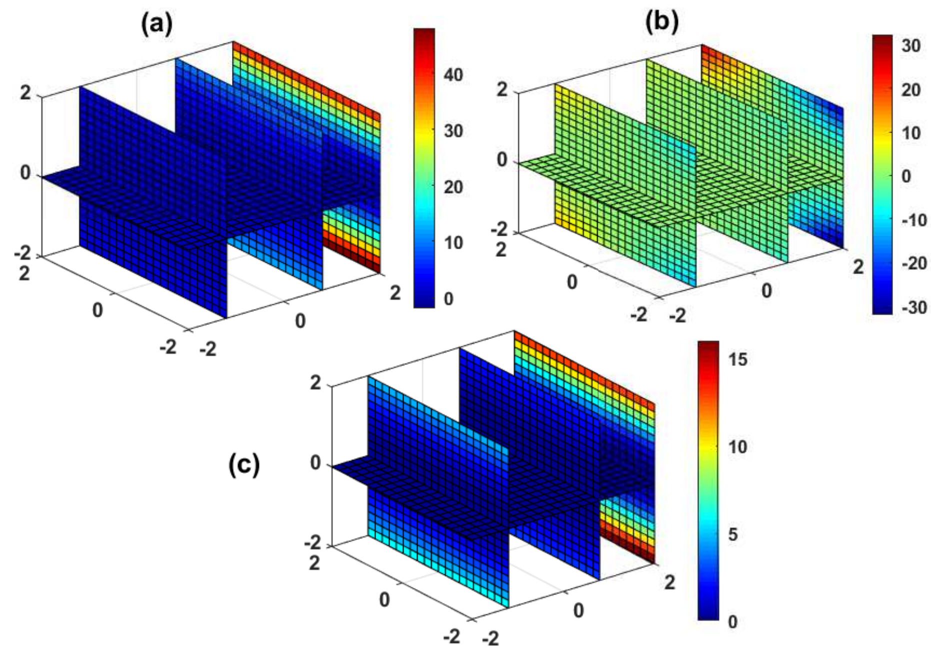

Figure 11: Complexity description of (a) ICA, (b) SOBI and (c) joint diagonalization methods

6. A note on computational complexity

SOBI has emerged as a reliable technique for modal recovery within the framework of BSS in structural identification problems (Hazra et al. (2009)). However, developing and implementing an online variant of SOBI – hypothetically termed recursive second-order blind identification (RSOBI) – in real-time is not feasible. This is mainly due to two reasons: (a) its inherent unitary factorization formulation, which is incompatible with FOEP (or HOP) and (b) the computational burden associated with simultaneous diagonalization tracking, which requires a parent loop-control structure and makes the investigation offline. Therefore, it is necessary to examine the computational cost of ICA, SOBI, and joint diagonalization approaches for modal identification (Shwartz et al. (2004)), as presented in Table 2.

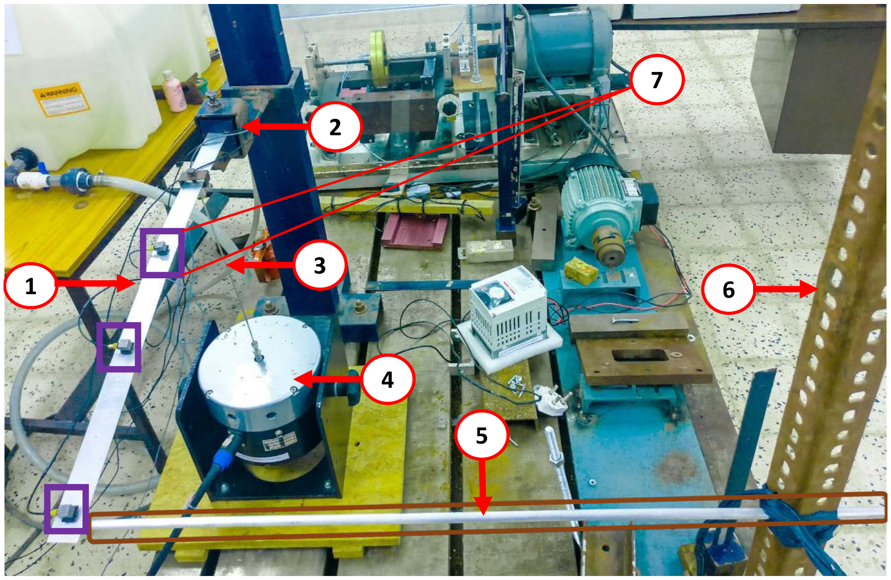

Figure 12: Vibro-impact experimental setup: 1–Aluminium beam. 2–Horizontal clamp. 3–Push-rod/stinger. 4–Shaker. 5–Impactor. 6–Vertical clamp. 7–Accelerometers (3)

Table 2: Summary of computational load for modal identification methods

Method	Complexity order	Approximate # Flops
ICA	$2d\,(d+1)\,\mathcal{O}\left(n^2\right)$	$0.8M^2T\left(N^2\right)$
SOBI	$d^2\mathcal{O}\left(ln^2\right)$	$T\,\left(2.5N^2\right)$
Joint diagonalization	$d^2\mathcal{O}\left(n^2\right)$	$\left(N^3-M^3\right)^2N^2$

For an easy comprehension of the expressions provided in Table 2, **Appendix C** provides an in-depth discussion on the empirically estimated parameters M, N and T. The computational complexity of the algorithms is characterized by parameters such as the number of monitored degrees of freedom (d), the number of lags (l) for SOBI, and the number of operations associated with estimating the eigenspace (n). From Table 2, it is evident that ICA is the most computationally expensive algorithm, followed by SOBI and joint diagonalization. ICA, being a fixed-point iteration algorithm, is complex to implement and requires a large number of operations. SOBI considers memory overhead but its implementation with a parent loop-control structure hinders real-time functionality. The proposed joint diagonalization algorithm is the most efficient in extracting modal information due to its simultaneous diagonalization and step-wise estimation operations. Appendix C provides a detailed analysis comparing the algorithms based on floating-point operations (flops), which serves as a fair metric for comparison. The analysis shows that the number of flops follows a similar pattern for each complexity order (Comon and Jutten (2010), with joint diagonalization requiring the fewest flops, followed by SOBI, and ICA requiring the most operations for modal identification.

The complexity assessment in Figure 11 clearly demonstrates the higher normalized expense for ICA. While most of the SOBI method is optimized for sequential iterations, the inclusion of an outer looping structure makes it the next complex approach. On the other hand, the simultaneous diagonalization of covariance matrices reduces the computational burden, making the proposed method a rational solution for modal recovery. Therefore, this investigation firmly establishes the execution of the proposed method as an efficient and viable alternative for real-time modal identification of dynamic systems.

7. Experimental verifications

Vibro-impact systems play a crucial role in various engineering applications, such as heat exchanger tubes, turbines, and offshore structures. These systems undergo a transition from a linear to a nonlinear state with each impact, resulting in contact nonlinearity (Chen et al. (2014)). To investigate this state transition in real-time, an experimental study was conducted using a vibrating system. Figure 12 illustrates the setup, which consists of an aluminium beam with a steel impactor attached at the free end. The assembly is placed on an immovable bench to prevent sliding during vibration testing. Three accelerometers fixed on the beam record the streaming data, which is utilized for state transition detection. In the experiment, the aluminium beam is excited using a scaled (70%) Gaussian white noise. Initially, the impactor is positioned 5mm away from the beam's stationary position, and this gap is maintained for the first 25s of excitation. Subsequently, the impactor is gradually slid, resulting in a series of repeated non-periodic impacts on the beam. With each impact, the gap size decreases until the beam and impactor behave as a rigid body system. The experiment continues for a total duration of 50s.

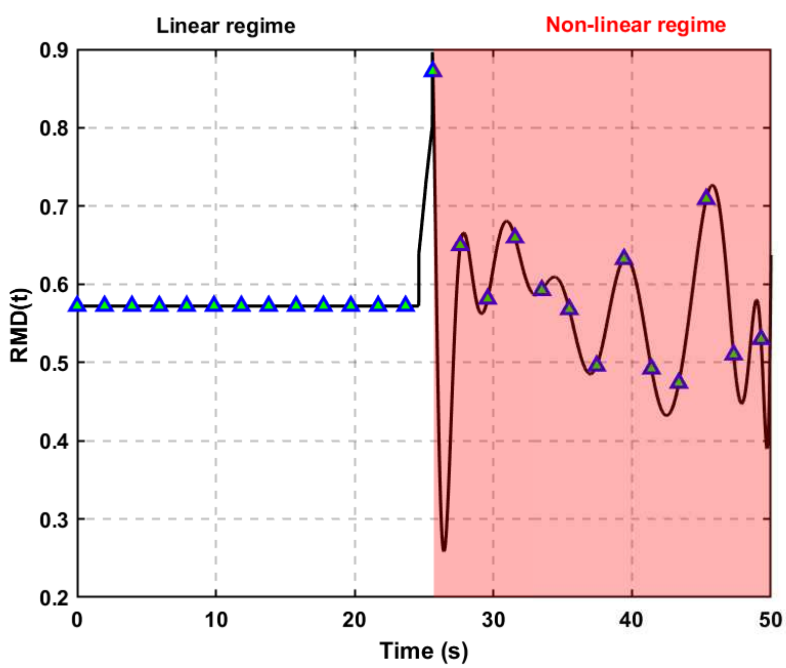

Figure 13: Real-time change of state detection

In real-time, the proposed method performs joint diagonalization of the covariance matrices at each time lag to track the eigenspace and detect the transition from a linear to a nonlinear state. Previous studies (Yeager et al. (2019); Tripura et al. (2020)) have shown the effectiveness of the

Mahalanobis distance as a metric for change detection in this context. Towards this, the present study develops a new recursive condition indicator – namely, *recursive Mahalanobis distance* – that takes into consideration the modal vibratory responses instead of the physical outputs within the ambit of generalized eigenvalue decomposition. Unlike previous approaches, this indicator considers the modal vibratory responses instead of physical outputs, using generalized eigenvalue decomposition. The theoretical development of this real-time indicator is provided in **Appendix B**. For a different derivation of this metric, readers can refer to Tripura et al. (2020). The experimental results depicted in Figure 13 clearly demonstrate a noticeable distortion in the mean level at 25s, indicating the onset of the state transition. The amplitude of the plot gradually decays over time but experiences a sudden increase towards the end of the excitation. This behavior is attributed to the near rigid body motion of the beam and impactor, which persists until the end of the experiment. The study conclusively demonstrates that the proposed methodology can effectively identify state changes in real-time for vibrating systems, particularly in offshore structures during seismic activities or wave surges.

8. Practical studies

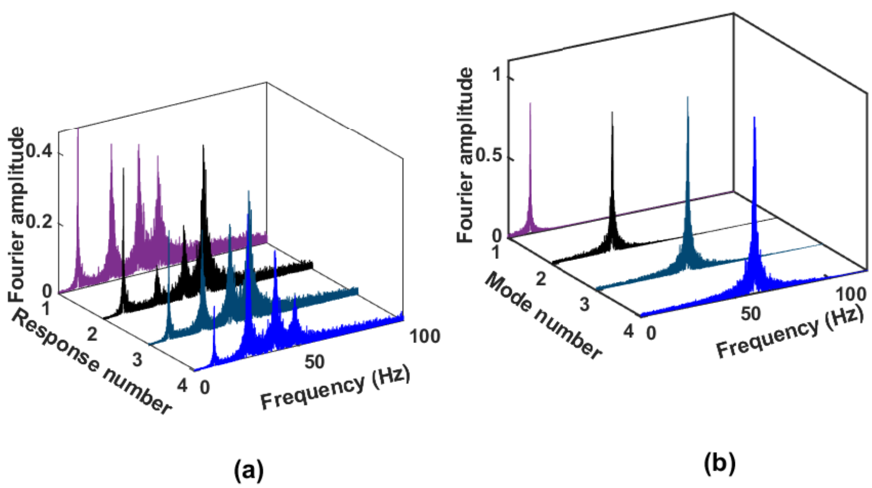

Figure 14: Combined spectral representation in (a) physical and (b) modal domain for the ASCE-SHM benchmark

The proposed method for online identification of vibratory modes is evaluated using the Phase-I IASC-ASCE SHM system benchmark (Johnson et al. (2004)). This benchmark consists of a quarter-scale steel frame structure with four stories and a 2.5m square base, modeled as a 12-DOF shear-building system (Caicedo et al. (2004)). The translational components (X and Y) and a rotation (θ) about the center column are considered, resulting in a 3-DOF per floor level representation. The undamaged state of the benchmark, corresponding to ID-0, is used for modal parameter estimation

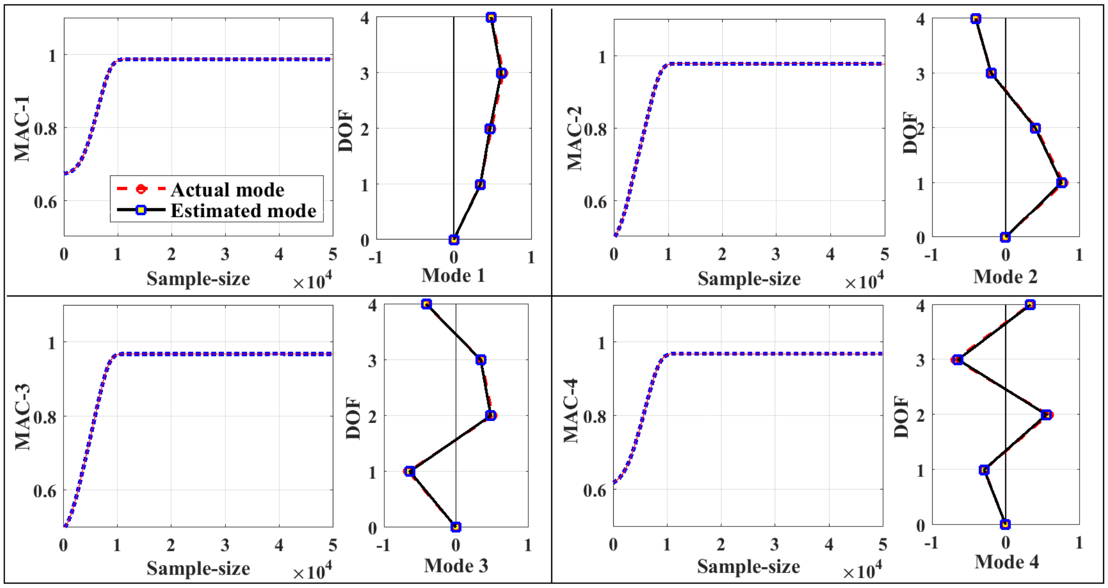

Figure 15: Recursive evolution of MAC across samples for ASCE-SHM benchmark

Table 3: Recursive MAC for IASC–ASCE benchmark

$\mathbf{i}^{th}$ Sample	MAC ϕ_1	ϕ_2	ϕ_3	ϕ_4
1000	0.6996	0.5869	0.5275	0.6296
2000	0.7571	0.7292	0.5812	0.6540
5000	0.9385	0.8619	0.7142	0.7455
10000	0.9911	0.9902	0.9591	0.9998
15000	0.9946	0.9985	0.9995	0.9987

ϕ_i represents the i^{th}corresponding modes

(Caicedo et al. (2004)). Gaussian white noise is applied as excitation in the positive Y direction on each floor slab. The sensor noise is assumed to be 10% of the maximum RMS value of the acceleration responses. The structure is simulated for 100s at a sampling rate of 500Hz, with a damping ratio of 2% critical in each mode. The frequency components obtained from the response signals are analyzed spectrally, as shown in Figure 14(a). The proposed method is then used to separate the modes, as depicted in Figure 14(b). Both subplots reveal a dominant spectral content up to 50 Hz for the first four modes of vibration.

In real-time, the streaming acceleration data undergoes prewhitening, and the time lagged covariance matrices are jointly diagonalized at each non-zero lag using FOEP. This process yields eigenspace estimates that are continuously tracked for modal recovery. The results of mode identification are depicted in Figure 15, where the recursive MAC values consistently converge to unity as the number of samples increases. This convergence, achieved at approximately 20% of the sample population, demonstrates accurate correlation with the theoretical modes. The subplots in Figure 15 further illustrate the near-perfect recovery of vibratory modes in real-time. The effectiveness of the proposed algorithm is also supported by the MAC values of each mode at pre-selected windows, as presented in Table 3,

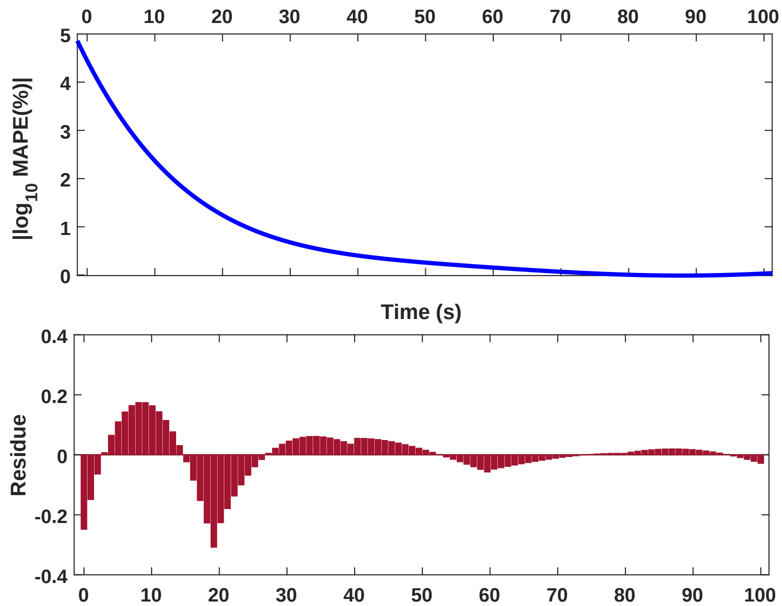

Figure 16: MAPE and residual error plots for the ASCE-SHM benchmark

where the MAC values exhibit consistent convergence with the increasing number of samples.

Furthermore, the convergence of the estimated eigenspace is analyzed in terms of error and is shown in Figure 16. The asymptotic curve starting from 20s indicates the attenuation of error, affirming the established convergence criteria of this study. The residual plot in the same figure demonstrates a noticeable reduction in error from 20s onwards, indicating diminishing discrepancies between the obtained eigenspace and theoretical modes. This investigation solidly establishes the proposed algorithm as an ideal choice for health monitoring applications in built infrastructure. The computational efficiency and real-time identification capabilities of the algorithm make it highly significant for both asset managers and infrastructure owners, particularly considering the time-varying behavior of vibratory systems.

9. Summary and conclusions

This paper introduces a novel framework for real-time blind modal identification using a single-step simultaneous diagonalization approach. The proposed method addresses the generalized eigenvalue decomposition problem within the first order eigen perturbation framework, eliminating the need for the two-step technique employed by traditional blind source separation methods. By recursively implementing integral pre-whitening, the method offers a computationally efficient solution for the subsequent eigenvalue decomposition problem. The approach simplifies computation, overcomes limitations of traditional independent component analysis (ICA) based methods, and eliminates the dependency on non-Gaussianity maximization.

The metric chosen for assessing modal consistency is the real-time modal assurance criteria (R-MAC), which demonstrates excellent convergence with approximately 20% of the sample size. This is particularly valuable when dealing with limited measurements due to sensor malfunctioning, power source issues, or remote monitoring challenges. The method also addresses the decentralized modal identification problem by achieving near-perfect modal recovery in real-time using a partial set of sensor responses.

The computational efficiency of the proposed method surpasses traditional ICA and second order blind identification (SOBI) methods by leveraging the recursive structure. Experimental tests conducted in a controlled environment validate the robustness of the method. Additionally, the development of the recursive Mahalanobis distance (RMD) serves as an online metric for real-time change detection.

Benchmark modal identification studies on the phase-I ASCE-SHM structure further demonstrate the applicability of the proposed approach. An error convergence analysis indicates a diminishing trend in error over time, confirming the effectiveness of the recursive simultaneous diagonalization method. Overall, the proposed method emerges as a favorable candidate for online monitoring of built infrastructure.

10. Discussions

The field of real-time modal identification techniques for dynamic systems presents significant challenges in the context of nonlinear systems, remote monitoring, and optimal sensor placement. In this comprehensive exploration, the findings have shed light on the limitations of existing numerical and experimental approaches, particularly in dealing with nonlinear systems and addressing challenges related to remote monitoring and optimal sensor placement. Based on the key findings of this research, the following research problems seem a natural extension of this work:

1. Enhancing Nonlinear Mode Recovery: Although the proposed method addresses the challenge of nonlinear mode recovery to some extent, further investigation can be done to improve the accuracy and robustness in scenarios with high damping or complex nonlinear behavior. This could involve exploring advanced techniques such as higher-order perturbation methods or machine learning algorithms to better handle nonlinearities and improve the completeness of modal recovery.

2. Adaptive Parameter Estimation: The proposed method assumes a known damping ratio and excitation characteristics. However, in real-world scenarios, these parameters may vary or be unknown. Research can be conducted to develop adaptive algorithms that can estimate the system parameters in real-time, allowing the method to adapt to changing conditions and improve the accuracy of modal identification.

3. Online Fault Detection and Diagnosis: While the proposed method incorporates the recursive Mahalanobis distance for real-time change detection, further research can be done to expand its capabilities for fault detection and diagnosis. This could involve developing algorithms that can distinguish between different types of faults or anomalies in the system based on the modal response patterns. Integration with advanced machine learning techniques, such as anomaly detection algorithms or pattern recognition methods, could enhance the fault detection and diagnosis capabilities.

4. Scalability for Large-Scale Structures: The proposed method has shown promising results in benchmark studies and experimental test beds. However, its scalability to large-scale structures with a high number of degrees of freedom remains an open research problem. Investigating techniques to handle the computational and data processing challenges associated with large-scale systems would be valuable. This could include exploring parallel computing, distributed algorithms, or model reduction techniques to enable efficient real-time modal identification for complex structures.

5. Integration with Sensor Placement Optimization: Sensor placement plays a crucial role in effective modal identification. Research can be conducted to integrate the proposed method with sensor placement optimization algorithms. This would allow for optimal selection of sensor locations that maximize the observability and accuracy of modal identification in real-time. Such integration could enhance the efficiency and cost-effectiveness of structural health monitoring systems.

11. Appendix A

Lemma 1: If $\mathbf{F} \in \Re^{n\times n}$ and $\left\|\mathbf{F}\right\|_p < 1$, then $\mathbf{I}-\mathbf{F}$ is nonsingular and

$$\left(\mathbf{I}-\mathbf{F}\right)^{-1} = \sum_{k=0}^{\infty} \mathbf{F}^k \tag{33}$$

with,

$$\left\|\left(\mathbf{I}-\mathbf{F}\right)^{-1}\right\|_p \leq \frac{1}{1-\left\|\mathbf{F}\right\|_p} \tag{34}$$

Proof: The proof starts with considering a contradiction that $(\mathbf{I}-\mathbf{F})$ is singular - which establishes that $(\mathbf{I}-\mathbf{F})\,x = 0$ for any nonzero x. This means that $\left\|x\right\|_p = \left\|\mathbf{F}x\right\|_p$ suggesting that $\left\|\mathbf{F}\right\|_p \geq 1$ – a contradiction. Therefore, $\mathbf{I}-\mathbf{F}$ is nonsingular. The inverse of the matrix can be obtained by considering the identity:

$$\left(\sum_{k=0}^{N} \mathbf{F}^k\right)(\mathbf{I}-\mathbf{F}) = \mathbf{I}-\mathbf{F}^{N+1} \tag{35}$$

Since $\|\mathbf{F}\|_p < 1$, it follows that $\lim_{k\to\infty} \mathbf{F}^k = 0$ as $\|\mathbf{F}_k\|_p \le \|\mathbf{F}\|_p^k$. Therefore, the following equation holds.

$$\left(\lim_{N\to\infty} \sum_{k=0}^{N} \mathbf{F}^k\right)(\mathbf{I}-\mathbf{F}) = \mathbf{I} \tag{36}$$

It follows that$(\mathbf{I}-\mathbf{F})^{-1} = \lim_{N\to\infty} \sum_{k=0}^{N} \mathbf{F}^k$. The proof of this lemma can be concluded by easily manifesting the equation in the form:

$$\left\|(\mathbf{I}-\mathbf{F})^{-1}\right\|_p \le \sum_{k=0}^{\infty} \|\mathbf{F}\|_p^k = \frac{1}{1-\|\mathbf{F}\|_p} \tag{37}$$

12. Appendix B

Recursive Mahalanobis Distance: Theoretical derivation

The traditional Mahalanobis distance metric is given by:

$$MD(X,t) = \sqrt{[X(t)-\mu_X(t)]^T \mathbf{\Sigma}_\mathbf{X}^{-1}(t)\,[X(t)-\mu_X(t)]} \tag{38}$$

where, $X(t)$ is a data vector with mean $\mu_X(t)$ and covariance matrix $\mathbf{\Sigma_X(t)}$. The physical responses of a vibratory system is related to responses in the modal coordinates $\mathbf{Z}$ through the covariance matrix $\mathbf{\Phi}$, as:

$$\mathbf{X} = \mathbf{\Phi Z} \;\Rightarrow\; \mathbf{Z} = \mathbf{\Phi}^{-1}\mathbf{X} = \mathbf{\Phi}^T\mathbf{X} \tag{39}$$

Consider a data stream evolving over time. The mean at any sample point k, is related to the mean at the previous sample $(k-1)$:

$$\mu_k = \frac{1}{k}\left(\sum_{i=1}^{k-1} X_i + X_k\right) \tag{40}$$

The covariance estimate at the $(k-1)^{th}$ sample is given as:

$$\begin{aligned}
\mathbf{\Sigma}_Z(k-1) &= \tfrac{k-2}{k-1}\mathbf{\Sigma}_Z(k-2) + \tfrac{1}{k-1}\begin{bmatrix} 0 & \mathbf{\Phi}^T\hat{X}_k\hat{X}_{k,\tau}^T\mathbf{\Phi} \\ \mathbf{\Phi}^T\hat{X}_{k,\tau}\hat{X}_k^T\mathbf{\Phi} & 0 \end{bmatrix} \\
&= \tfrac{k-2}{k-1}\mathbf{\Sigma}_Z(k-2) + \tfrac{1}{k-1}\begin{bmatrix} 0 & \mathbf{\Phi}^T\hat{\mathbf{R}}_{X,k}\mathbf{\Phi} \\ \mathbf{\Phi}^T\hat{\mathbf{R}}_{X,k}\mathbf{\Phi} & 0 \end{bmatrix} \\
&= \mathbf{P} + \mathbf{QU}
\end{aligned} \tag{41}$$

The above form of the equation typically resembles the structure where Woodbury's theorem can be put into use. Examining the structure of the $\mathbf{QU}$ matrix, one obtains:

$$\mathbf{QU} = \frac{1}{k-1}\begin{bmatrix} 0 & \mathbf{\Phi}^T\hat{X}_k \\ \mathbf{\Phi}^T\hat{X}_{k,\tau} & 0 \end{bmatrix}\begin{bmatrix} \hat{X}_{k,\tau}^T\mathbf{\Phi}^T & 0 \\ 0 & \hat{X}_{k,\tau}^T\mathbf{\Phi}^T \end{bmatrix} \tag{42}$$

Substituting in Eq. 41 and employing the Woodbury's identity for the generalized inversion of a matrix:

$$\begin{aligned}\boldsymbol{\Sigma}_Z^{-1}(k-1) &= \left[\mathbf{P}(k+1) + \mathbf{Q}(k+1)\mathbf{U}(k+1)\right]^{-1} \\ &= \mathbf{P}^{-1}(k+1) - \mathbf{P}^{-1}(k+1)\mathbf{Q}(k+1)\left[\mathbf{U}^{-1}(k+1) + \mathbf{P}^{-1}(k+1)\mathbf{Q}(k+1)\right]^{-1}\mathbf{P}^{-1}(k+1)\end{aligned} \tag{43}$$

The following recursive formulation of the Mahalanobis distance is therefore, obtained:

$$RMD(X,k) = \left|\sqrt{\left[\boldsymbol{\Phi}^T X(k) - \mu_{\Phi,X}(k)\right]^T \boldsymbol{\Sigma}_Z^{-1}(k-1)\left[\boldsymbol{\Phi}^T X(k) - \mu_{\Phi,X}(k)\right]}\right| \tag{44}$$

13. Appendix C

This section aims at giving insights into the numerical complexity of algorithms discussed in this work, as a function of the number of sources (N), the number of sensors (P) and the data length (T). Considering the linear 5DOF system, $N = P = 5$, $T = 10000$ data samples with two matrices diagonalized at each stage (M).

According to Comon and Jutten (2010), the number of flops for the ICA algorithm is given as:

$$ICA|_{flops} = \min\left(TP^2/2 + 4P^3/3 + NPT,\ 2TP^2\right) + P^3 + \left(16N^3/3 + N^2 + 3TN^2\right) \tag{45}$$

On substituting the values, the number of flops required for ICA is obtained as:

$$ICA|_{flops} = \mathbf{800817} \approx 0.8M^2T\left(N^2\right) \tag{46}$$

For the SOBI method, the number of flops can be represented through the equation:

$$SOBI|_{flops} = MTP^2/2 + 4P^3/3 + (M-1)P^3/2 + IN(N-1)\left[17(M-1) + 75 + 4N + 4NM\right]/2 \tag{47}$$

Here, $I = 2N^3$ (Mucchielli et al. (2020)). With proper substitution, a compact form can be arrived as:

$$SOBI|_{flops} = \mathbf{630230} \approx T\left(2.5N^2\right) \tag{48}$$

Similarly, Comon and Jutten (2010) also provides a rough estimation involving the number of flops for a simultaneous joint diagonalization approach. With minimal modifications in the formulation, the expression for the number of flops for the proposed method can be given by:

$$\begin{aligned}JAD|_{flops}^{proposed} &= \min\left(TP^2/2 + 4P^3/3 + NPT,\ 2TP^2\right) + TN^2 + \min\left(4N^6/3,\ 8N^3\left(N^2+3\right)\right) \\ &\quad + N(N-1)\left(75 + 21N + 4N^2\right)/2\end{aligned} \tag{49}$$

Condensing the terms here after proper substitution, the adjusted expression holds as:

$$JAD|_{flops}^{proposed} = \mathbf{323634} \approx \left(N^3 - M^3\right)^2 N^2 \tag{50}$$

This investigation leads to the belief that the number of flops for the proposed algorithms is the least, in comparison to traditional SOBI and ICA based approaches.

Acknowledgements

Basuraj Bhowmik gratefully acknowledges the support received in the form of Seed Grant from the Indian Institute of Technology (BHU), Varanasi.

References

Amini, F., Ghasemi, V., 2018. Adaptive modal identification of structures with equivariant adaptive separation via independence approach. Journal of Sound and Vibration 413, 66–78.

Antoni, J., Chauhan, S., 2013. A study and extension of second-order blind source separation to operational modal analysis. Journal of Sound and Vibration 332, 1079–1106.

Bhowmik, B., Hazra, B., Pakrashi, V., 2022. Real-time Structural Health Monitoring of Vibrating Systems. CRC Press.

Bhowmik, B., Krishnan, M., Hazra, B., Pakrashi, V., 2019a. Real-time unified single-and multi-channel structural damage detection using recursive singular spectrum analysis. Structural Health Monitoring 18, 563–589.

Bhowmik, B., Tripura, T., Hazra, B., Pakrashi, V., 2019b. First order eigen perturbation techniques for real time damage detection of vibrating systems: Theory and applications. Applied Mechanics Reviews 71.

Bhowmik, B., Tripura, T., Hazra, B., Pakrashi, V., 2020. Robust linear and nonlinear structural damage detection using recursive canonical correlation analysis. Mechanical Systems and Signal Processing 136, 106499.

Caicedo, J.M., Dyke, S.J., Johnson, E.A., 2004. Natural excitation technique and eigensystem realization algorithm for phase i of the iasc-asce benchmark problem: Simulated data. Journal of Engineering Mechanics 130, 49–60.

Chandola, V., Banerjee, A., Kumar, V., 2009. Anomaly detection: A survey. ACM computing surveys (CSUR) 41, 1–58.

Chen, H., Kurt, M., Lee, Y.S., McFarland, D.M., Bergman, L.A., Vakakis, A.F., 2014. Experimental system identification of the dynamics of a vibro-impact beam with a view towards structural health monitoring and damage detection. Mechanical Systems and Signal Processing 46, 91–113.

Cichocki, A., Amari, S.i., 2002. Adaptive blind signal and image processing: learning algorithms and applications. John Wiley & Sons.

Comon, P., Jutten, C., 2010. Handbook of Blind Source Separation: Independent component analysis and applications. Academic press.

Feeny, B., Liang, Y., 2003. Interpreting proper orthogonal modes of randomly excited vibration systems. Journal of Sound and Vibration 265, 953–966.

Gao, Y., Spencer Jr, B., Ruiz-Sandoval, M., 2006. Distributed computing strategy for structural health monitoring. Structural Control and Health Monitoring: The Official Journal of the International Association for Structural Control and Monitoring and of the European Association for the Control of Structures 13, 488–507.

Hazra, B., Roffel, A., Narasimhan, S., Pandey, M., 2009. Modified cross-correlation method for the blind identification of structures. Journal of Engineering Mechanics 136, 889–897.

Hazra, B., Sadhu, A., Roffel, A.J., Narasimhan, S., 2012. Hybrid time-frequency blind source separation towards ambient system identification of structures. Computer-Aided Civil and Infrastructure Engineering 27, 314–332.

Hyvärinen, A., Oja, E., 2000. Independent component analysis: algorithms and applications. Neural networks 13, 411–430.

James, G., Carne, T.G., Lauffer, J.P., et al., 1995. The natural excitation technique (next) for modal parameter extraction from operating structures. Modal Analysis-the International Journal of Analytical and Experimental Modal Analysis 10, 260.

Johnson, E.A., Lam, H.F., Katafygiotis, L.S., Beck, J.L., 2004. Phase i iasc-asce structural health monitoring benchmark problem using simulated data. Journal of engineering mechanics 130, 3–15.

Juang, J.N., Pappa, R.S., 1985. An eigensystem realization algorithm for modal parameter identification and model reduction. Journal of guidance, control, and dynamics 8, 620–627.

Kerschen, G., Golinval, J.C., 2002. Physical interpretation of the proper orthogonal modes using the singular value decomposition. Journal of Sound and vibration 249, 849–865.

Krishnan, M., Bhowmik, B., Hazra, B., Pakrashi, V., 2018. Real time damage detection using recursive principal components and time varying auto-regressive modeling. Mechanical Systems and Signal Processing 101, 549–574.

Krishnan, M., Bhowmik, B., Tiwari, A., Hazra, B., 2017. Online damage detection using recursive principal component analysis and recursive condition indicators. Smart Materials and Structures 26, 085017.

McNeill, S., Zimmerman, D., 2008. A framework for blind modal identification using joint approximate diagonalization. Mechanical Systems and Signal Processing 22, 1526–1548.

Mucchielli, P., Bhowmik, B., Hazra, B., Pakrashi, V., 2020. Higher-order stabilized perturbation for recursive eigen-decomposition estimation. Journal of Vibration and Acoustics 142.

Parra, L., Sajda, P., 2003. Blind source separation via generalized eigenvalue decomposition. Journal of Machine Learning Research 4, 1261–1269.

Poncelet, F., Kerschen, G., Golinval, J.C., Verhelst, D., 2007. Output-only modal analysis using blind source separation techniques. Mechanical systems and signal processing 21, 2335–2358.

Ren, W.X., De Roeck, G., 2002. Structural damage identification using modal data. i: Simulation verification. Journal of Structural Engineering 128, 87–95.

Rofooei, F., Mobarake, A., Ahmadi, G., 2001. Generation of artificial earthquake records with a nonstationary kanai–tajimi model. Engineering Structures 23, 827–837.

Shwartz, S., Zibulevsky, M., Schechner, Y.Y., 2004. Ica using kernel entropy estimation with nlogn complexity, in: International Conference on Independent Component Analysis and Signal Separation, Springer. pp. 422–429.

Skolnik, D., Lei, Y., Yu, E., Wallace, J.W., 2006. Identification, model updating, and response prediction of an instrumented 15-story steel-frame building. Earthquake Spectra 22, 781–802.

Stewart, G.W., 1998. Perturbation theory for the singular value decomposition. Technical Report.

Tripura, T., Bhowmik, B., Pakrashi, V., Hazra, B., 2020. Real-time damage detection of degrading systems. Structural Health Monitoring 19, 810–837.

Yang, Y., Nagarajaiah, S., 2014. Blind identification of damage in time-varying systems using independent component analysis with wavelet transform. mechanical systems and signal processing 47, 3–20.

Yeager, M., Gregory, B., Key, C., Todd, M., 2019. On using robust mahalanobis distance estimations for feature discrimination in a damage detection scenario. Structural Health Monitoring 18, 245–253.

Zhou, W., Chelidze, D., 2007. Blind source separation based vibration mode identification. Mechanical systems and signal processing 21, 3072–3087.

Zimmerman, A.T., Shiraishi, M., Swartz, R.A., Lynch, J.P., 2008. Automated modal parameter estimation by parallel processing within wireless monitoring systems. Journal of Infrastructure Systems 14, 102–113.